Ultramicroelectrodes in Electrochemistry

By Jürgen Heinze*

Dedicated to Professor Herbert Zimmermann on the occasion of his 65th birthday

In the 1950s and 1960s fundamental developments in electrochemical methods included voltammetry and low signal techniques. A generation later, the discovery of the unusual properties of ultramicroelectrodes has opened new possibilities of analyzing electrode processes. The changes in mass transport conditions bring about extremely high current densities at ultramicroelectrodes, whereas the currents themselves become very small. This little-noticed phenomenon allows for many electroanalytical applications that are not possible with conventional electrodes, especially experiments in solutions with very low electrolyte concentrations, in nonpolar solvents, in solids, and even in gases. In addition, two factors—changes in the experimental time scale at low scan rates because of the size of the electrode, and insignificant *iR* effects at very high scan rates—make it possible to study very fast homogeneous and heterogeneous electrode processes.

1. Introduction

Electrodes are systems of coupled electrically conducting phases, which are usually in electrochemical equilibrium. An exchange of charges takes place across the interfaces between the phases. The reaction at the phase interface is known as an electrode reaction, and the exchange of charged particles across the phase interface is a charge transfer reaction. As a rule, one phase conducts electrons and at least one phase ions (metal or semiconductor electrode). In principle, an electrode can also consist of two ion-conducting phases.

In textbooks, some such definition will introduce the electrode as the crucial instrument of electrochemistry. Accordingly, almost all our knowledge in this field concerns electrodes directly or indirectly. In basic research, electrode kinetics[1] and electrochemical thermodynamics provide comprehensive theories that are continually being extended to explain the properties of electrodes and the processes at or through them. Hence, it comes as a surprise to learn that in the past electrochemists paid little attention to the influence that size and geometry of the electrode surface have on electrochemical processes, apart from the direct proportionality between size and the measured signal.[2]

The development of polarography[3] made the relatively small spherical Hg drop electrode widely known as early as 1922. Initially, however, no one appears to have obtained theoretical or experimental findings that indicated a direct relationship between the size of the drop and its electrochemical properties. In 1937 MacGillavry and Rideal[4] set up a current–time equation for the stationary, spherical electrode for the first time, which predicted that the course of the diffusion-controlled current over time depended on the size of the radius. Two years later, Laitinen and Kolthoff were unable to verify this relationship experimentally.[5a] In 1941 the same authors reported the results of voltammetric experiments using thin wire electrodes.[5b] They interpreted the stationary currents they observed as a consequence of natural convection, and did not relate them to surface size or geometry of the electrode. Only in the mid 1960s, when current–time measurements at small stationary disk electrodes excluded the influence of convection, was it accepted that the results did not agree with the theory of planar diffusion. These phenomena were interpreted as edge effects due to surface size, for the most part the result of quasi-spherical diffusion processes.[6] At about this time, almost twenty-five years after it had been theoretically predicted, experiments confirmed for the first time that the current response in chronoamperometric experiments with spherical electrodes becomes time-independent and stationary. The time lapse before the stationary value is attained depends on the electrode radius.[7] Although the subject attracted some interest in the following years,[8–7] only at the end of the 1970s did Fleischmann and co-workers at the University of Southampton[18] establish beyond question that diminishing electrode surface size has not only quantitative effects, but also—and always—unusual qualitative effects.[19, 20] For instance, chronoamperometric measurements at electrodes with μm dimensions (≤ 20 μm) showed that, in contradiction of Cottrell's theory,[21] even with planar electrodes a time-independent stationary state is reached very rapidly. Other conspicuous phenomena included high current densities in spite of small measuring currents, the possibility of measuring transients at considerably shorter time scales as well as a drastic decrease in the ohmic drop caused by the resistance of the solution. In 1981 Wightman provided a first comprehensive survey of the special properties and perspectives of microvoltammetric electrodes.[22]

These discoveries have encouraged numerous research groups to study the properties and applications of ultramicroelectrodes in theory and practice.

The concept of ultramicroelectrodes (UME) is now a widely accepted term in the literature. However, unlike in the field of electrophysiology, in electrochemistry it is not necessary for all dimensions of probes to be extremely small. In principle, only one, the characteristic dimension that is given by the geometry of the electrode, must be very small. For instance, a very narrow, but long band electrode makes a suitable ultramicroelectrode.

In their enthusiasm, electrochemists should not forget that microelectrodes with diameters of 25 μm have long been

[*] Prof. Dr. J. Heinze
Institut für Physikalische Chemie der Universität
Albertstrasse 21, D-79104 Freiburg (FRG)
Telefax: Int. code + (761)203-2815

used in medical and biological research.[23] They were initially developed to determine the oxygen content of living tissue and tissue liquids.[24, 25] Accordingly, the electrodes had to be as small as possible. The users either did not notice the unconventional properties of these electrodes, or did not think anything of it.

Electrochemists are interested in ultramicroelectrodes mainly because their application in accordance with the general principles of practice used in voltammetry and chronoamperometry opens totally new possibilities for studying electrode reactions. The results of dynamic measurements in solvents with low electrolyte concentrations or in poorly conducting media,[26] or in the solid state,[27] or even in the gas phase[28] have been particularly spectacular. This will ensure that in future electrochemical data will be obtained under similar experimental conditions as, for example, in spectroscopy.

Moreover, using microelectrodes expands the time scale for measurements by several orders of magnitude, which makes it much easier to study rapid homogeneous or heterogeneous reactions with microelectrodes than with, for example, rotating electrodes. Over and above this, the combination of exceptionally high current densities and low measuring currents promises new applications in the fields of analysis, sensors, and scanning electrochemical microscopy.[29] At the same time, the small dimensions of the electrodes guarantee that the experiment will not alter or destroy the object measured, a very important aspect in, for instance, biophysical examinations.

A growing number of communications, progress reports,[30] and books[31] indicates that the above-mentioned set of examples is by no means complete. As ultramicroelectrodes become commercially available, this technique will soon find new friends outside specialized electrochemical laboratories. It is hoped that this survey will encourage this development.

2. Electrochemistry at Ultramicroelectrodes

2.1. Mass Transport

In principle, experiments using ultramicroelectrodes are similar to those using conventional electrodes. A stationary electrode immersed in an unstirred electrolytic solution is given either a constant potential or one that changes linearly over time. Provided there is an electroactive substance, that is, one that can undergo oxidation or reduction, in the electrolytic solution, a heterogeneous charge transfer will occur at the metal/liquid interface, during which, in the case of reduction, for example, electrons will be transferred from the electrode to the electroactive substance.[1, 32] At the same time, the concentrations at the electrode surface start to change, which sets off diffusive mass transport to and from the electrode.

Depending on the size of the electrode and the volume of electrolytic solution used, one can distinguish between three limiting cases of diffusion. The simplest case is an electrode in a thin-layer cell with a very low ratio of cell volume to electrode surface. Under these conditions, mass transport within the cell is negligible, and no diffusion gradient develops.[33] By reducing the ratio between the electrode surface and the electrolyte volume, one approximates the normal situation of a voltammetric experiment with semi-infinite planar diffusion.[34] With the transition to extremely small electrode surfaces, the conditions change yet again, and the diffusion process becomes dependent on the size and geometry of the electrode[2, 30, 31] (Fig. 1).

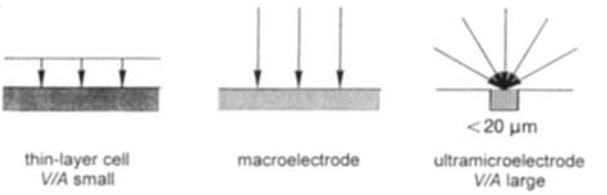

Fig. 1. Limiting cases of diffusive mass transport in electrochemical cells. Left: Thin-layer cell; the available transport paths are short, and no diffusion gradient develops. The ratio between electrolyte volume (V) and electrode area (A) is very low. Center: Macroelectrode (for example, disk with diameter ≥ 0.01 m); mass transport perpendicular to electrode is in form of a semi-infinite planar diffusion. In mathematical terms, the process corresponds to mass transport in a one-dimensional diffusion field [Eq. (1)]. Right: Ultramicroelectrode; the diffusion process depends on the shape of the electrode. A spatial diffusion field develops (hemispheric in the case of a disk electrode) [Eqs. (2–6)]. The V/A ratio is extremely high.

As one might expect, the voltammetric current–voltage curves of these three cases differ markedly. In the case of a thin electroactive layer, the cathodic and anodic waves appear as perfect mirror images. Normal electrodes produce the characteristic cyclic voltammograms,[34] and extremely

Jürgen Heinze was born in Dresden in 1939. He studied chemistry in Cologne and Munich from 1960 to 1966. After obtaining his Diploma, he completed a PhD under Herbert Zimmermann in Freiburg in 1971 on the synthesis and physical properties of azole systems. In 1980 he habilitated in Physical Chemistry with studies on microelectrodes and was appointed professor in 1987. Since 1991 he has been a member of the newly founded Freiburger Materialforschungszentrum. He is chairman of the Baden-Württemberg priority research program, "Electroactive Materials for Sensor Technology". His main research subjects are mechanistic investigations of electron-transfer-induced processes and their coupled chemical reactions, and the development of new and improved methods of electrode kinetics (cyclic voltammetry), in particular, those involving microelectrodes. Further interests include electroactive materials, such as conductive polymers, and the development of electrochemical sensors.

small electrodes (ultramicroelectrodes) yield steady-state current–voltage curves, which resemble the classic polarograms as well as the current–voltage curves of rotating electrodes (Fig. 2).

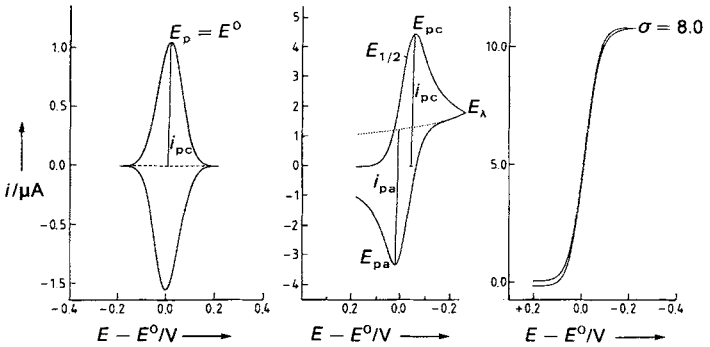

Fig. 2. Voltammetric current–voltage curves. Left: for the thin-layer cell; center: for semi-infinite planar diffusion ($\sigma = 0$) to a macroelectrode; right: for semi-infinite hemispheric diffusion to a microdisk electrode ($\sigma = 8.0$). E_λ = switching potential, $E_{\frac{1}{2}}$ = half-wave potential, E_p = peak potential, E_{pa} = anodic peak potential, E_{pc} = cathodic peak potential, i_{pa} = anodic peak current, i_{pc} = cathodic peak current. The V/A ratio increases from left to right.

The phenomena at ultramicroelectrodes are caused by time-dependent changes in mass transport, in which one-dimensional diffusion fields transform into spatial fields. In the case of planar electrodes, besides the usual axial diffusion, an additional, radial diffusive component becomes effective parallel to the electrode surface. In the case of curved electrode surfaces, spherical or cylindrical diffusion fields form over time at rates that depend on electrode size.

In mathematical terms, the diffusion is described by Fick's Laws, which vary for spatial fields [Eqs. (1–5)] according to the electrode geometry.[35]

$$\frac{\partial c}{\partial t} = D\frac{\partial^2 c}{\partial x^2} \qquad \text{(planar diffusion)} \qquad (1)$$

$$\frac{\partial c}{\partial t} = D\left(\frac{\partial^2 c}{\partial r^2} + \frac{1}{r}\frac{\partial c}{\partial r}\right) \qquad \text{(cylindrical electrode)} \qquad (2)$$

$$\frac{\partial c}{\partial t} = D\left(\frac{\partial^2 c}{\partial r^2} + \frac{2}{r}\frac{\partial c}{\partial r}\right) \qquad \text{(spherical electrode)} \qquad (3)$$

$$\frac{\partial c}{\partial t} = D\left(\frac{\partial^2 c}{\partial r^2} + \frac{1}{r}\frac{\partial c}{\partial r} + \frac{\partial^2 c}{\partial z^2}\right) \qquad \text{(disk)} \qquad (4)$$

$$\frac{\partial c}{\partial t} = D\left(\frac{\partial^2 c}{\partial x^2} + \frac{\partial^2 c}{\partial z^2}\right) \qquad \text{(band)} \qquad (5)$$

The introduction of further boundary conditions determines whether the diffusion will be finite (thin-layer cell) or semi-infinite and whether the electrode reaction will proceed galvanostatically (constant current), potentiostatically (constant potential), or potentiodynamically (variable potential). When ultramicroelectrodes are used, measurements are generally potentiostatic (chronoamperometry) or potentiodynamic (cyclic voltammetry).

The planar disk is the most popular electrode in experiments (Fig. 3). It is constructed relatively easily by encasing a metal wire or a carbon fiber in glass or embedding it in

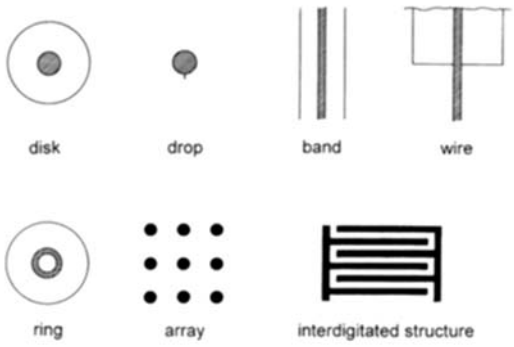

Fig. 3. Typical configurations of ultramicroelectrodes.

plastic; the flat surface of the end of the insulated wire serves as the active electrode surface.[6, 36–38] Recently, greater use has been made of band[39–42] and ring electrodes,[43, 44] whose surface areas can be enlarged by altering the length of the band or the circumference of the ring without losing the specific properties of ultramicroelectrodes. The same objective can be achieved with electrode arrays,[45–47] that is, several electrodes arranged, for example, in the form of an interdigitated structure. However, with arrays the diffusion conditions change depending on the arrangement of the electrodes. This means that, during very long experiments, the diffusion field eventually returns to a planar form.[48, 49] From a theoretical point of view, spherical (Hg drop)[49] and cylindrical (wire) electrodes[17, 41, 51] are particularly interesting, as they allow for one-dimensional solutions to the diffusion problem.[2, 4, 35]

2.2. Chronoamperometry

Notwithstanding different diffusion equations, when the surface area is reduced, qualitatively similar changes take place in the current response of all electrodes, irrespective of shape. This is because at electrodes generally the particle flux per surface unit increases as the distance from the electrode surface decreases. A study of chronoamperometric experiments reveals the details of this phenomenon.

In the simplest case of a chronoamperometric (potential step) experiment, a working electrode is given a potential sufficient to completely reduce or oxidize at the electrode surface a dissolved electroactive substance of concentration c^*. The corresponding initial and boundary conditions are compiled in Equations (6)–(8).

$$c(x,0) = c^* \qquad (t = 0) \qquad (6)$$

$$\lim_{x \to \infty} c(x,t) = c^* \qquad (t > 0) \qquad (7)$$

$$c(0,t) = 0 \qquad (8)$$

Experiment and theory show that under these conditions a diffusion-controlled, faradaic current i flows over the electrode. Its value (in A, proportional to j, the flux in $\mathrm{mol\,s^{-1}\,m^{-2}}$) is directly proportional to the concentration gradient at the electrode surface [Eq. (9), where F is the faradaic constant, D the diffusion coefficient, and A the area

$$\frac{i}{nFA} = j(0,t) = -D\left[\frac{\partial c}{\partial x}\right]_{x=0} \tag{9}$$

of the electrode]. This gradient causes the formation of a diffusion layer in front of the electrode, which gradually spreads into the solution (Fig. 4, top). For a purely planar

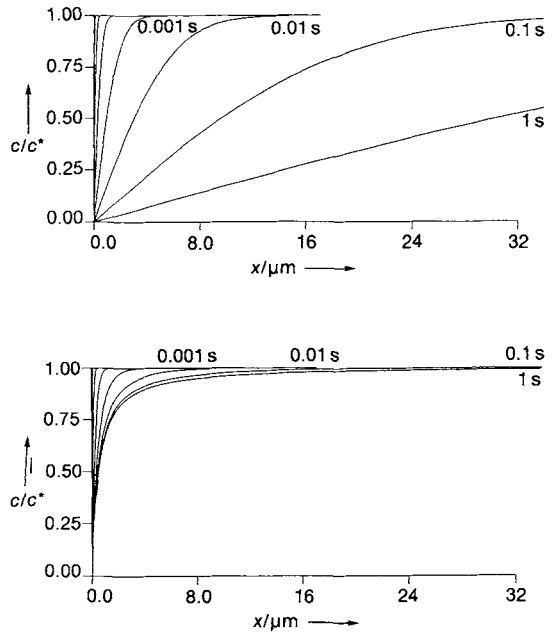

Fig. 4. Concentration profiles of diffusion layers (diffusion coefficient $D = 1 \times 10^{-9}\ m^2 s^{-1}$) in a chronoamperometric experiment for different times t after application of a potential step (concentration of the electroactive species at electrode surface is zero). Top: semi-infinite planar diffusion; bottom: spherical diffusion for a spherical microelectrode with $r_0 = 0.5$ μm. c/c^* = normed concentration, x = distance from electrode.

diffusion, the time-dependent current obeys the Cottrell equation [Eq. (10)],[21] which predicts that the current in

$$\frac{it^{1/2}}{nFAD^{1/2}c^*} = \frac{1}{\pi^{1/2}} \tag{10}$$

the chronoamperometric experiment is inversely proportional to $t^{\frac{1}{2}}$.

The conditions for planar diffusion are properly fulfilled only if the electrode surface is very large. In the case of a disk electrode, edge effects become increasingly noticeable as surface area decreases: in addition to the mass transport perpendicular to the electrode, mass transport also develops parallel to the electrode. The size of the edge effects depends on duration of the measurement and electrode radius. Figure 5 shows computed concentration profiles at disk electrodes with different radii recorded after 1 s of measuring.

From this it is clear that as the electrode radius decreases, semi-infinite planar diffusion gradually transforms into semi-infinite hemispherical diffusion. Longer experiment duration produces the same phenomenon. Due to the time-dependent change in the diffusion profile, the solid angle occupied by the diffusion layer in front of the electrode increases, and hence, grows considerably relative to the electrode surface. As a consequence, many more electroactive particles per unit time and area reach the electrode than in

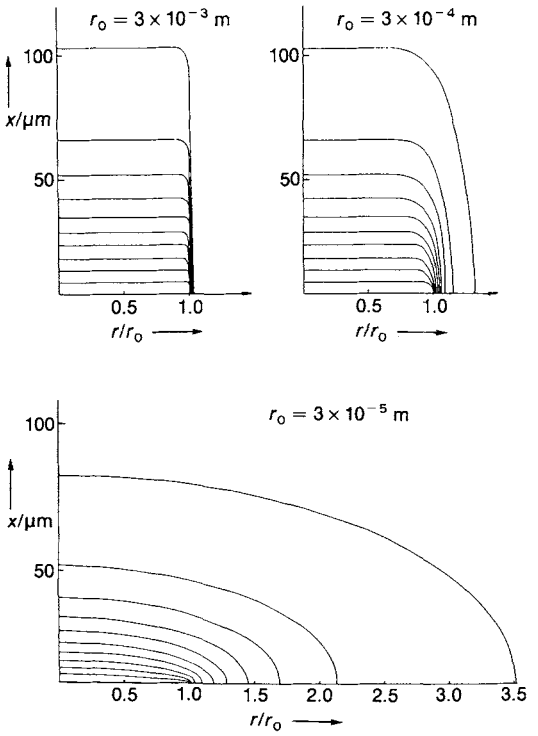

Fig. 5. Normalized calculated concentration profiles c/c^* calculated for disk electrodes with different radii ($r_0 = 3 \times 10^{-3}$, 3×10^{-4}, 3×10^{-5} m; $D = 1 \times 10^{-9}\ m^2 s^{-1}$) 1 s after start of a chronoamperometric experiment; concentration of the electroactive species at the electrode is zero because of a high potential pulse. Concentration curves are separated by 0.1 of a concentration unit. x = distance perpendicular to the electrode.

the case of pure planar diffusion. On the other hand, the growing volume within the prescribed solid angle means that the particle flux in and out of the volume eventually becomes stationary (Fig. 4b) and the diffusion layer stops growing. The mass transport rate in the stationary case is given by the mass transport coefficient m (in $m s^{-1}$). Its value in a (hemi)spherical field is indirectly proportional to the electrode radius r_0 [Eq. (11)]. Consequently, for extremely small electrodes the diffusion rate can be extraordinarily high.

$$m = Dr_0^{-1} \tag{11}$$

Hence, the calculation of the current–time curve produces a modified Cottrell equation [Eq. (12)]. For the disk elec-

$$\frac{it^{1/2}}{nFAD^{1/2}c^*} = \frac{1}{\pi^{1/2}}\left(1 + b\left(\frac{Dt}{r_0^2}\right)^{1/2}\right) \tag{12}$$

trode,[6, 13, 52] $\pi^{\frac{1}{2}} \leq b \leq 4\pi^{-\frac{1}{2}}$. The value of the prefactor b changes in the transition from the planar to the hemispherical diffusion field. Approximate formulas for this intermediate case may be found in the literature.[53, 54] By analogy, Equation (13) is valid for the spherical electrode.[2, 4] As long

$$\frac{it^{1/2}}{nFAD^{1/2}c^*} = \frac{1}{\pi^{1/2}}\left(1 + \pi^{1/2}\left(\frac{Dt}{r_0^2}\right)^{1/2}\right) \tag{13}$$

as planar diffusion dominates and the measuring time is short, the second term on the right-hand side of Equations (12) and (13) can be neglected, which results in the

limiting case of Equation (10). By contrast, if the measuring time is very long, the first term on the right-hand side becomes negligible, and the result is a stationary current. The smaller the electrode surface, the shorter the time lapse before the stationary state is established. The parameter (14)

$$\eta = \left(\frac{Dt}{r_0^2}\right)^{1/2} \tag{14}$$

characterizes the extent of the nonplanar diffusion. For values of η greater than 6, the current becomes stationary; for smaller values, one approximates the limiting case of planar diffusion. Oldham's comprehensive theoretical studies[55-57] have shown that one can set up an identity for the stationary limiting currents i_{Gr} (in A) for the spherical, hemispherical, and disk electrodes by introducing a surface diameter d [Eq. (15)]. For the sphere, $d = 2\pi r_0$, for the hemi-

$$i_{Gr} = 2nFc^*Dd \tag{15}$$

sphere $d = \pi r_0$, and for the disk electrode $d = 2r_0$. The attainable stationary limiting currents for the different electrode forms are listed in Table 1.[41,56-59] In contrast to

Table 1. Limiting currents for ultramicroelectrodes.

Sphere
$i_{Gr} = 4\pi r_0 nFDc^*$

Hemisphere
$i_{Gr} = 2\pi r_0 nFDc^*$

Disk:
$i_{Gr} = 4r_0 nFDc^*$
is identical with the sphere when = $(\pi/2)r_0$ (hemisphere)

Cylinder (approximate)
$i = 2nFADc^* \dfrac{1}{\ln[4(Dt)/r_0^2]}$
where A = cylinder surface area ($2\pi r_0 l$) or
hemicylinder surface area ($\pi r_0 l$), l = length of the cylinder

Band electrode (approximate)
$i = 2\pi nFDc^* l \dfrac{1}{\ln[4(Dt)/r_0^2]}$
l = length of the band

Ring
$\dfrac{\lim_{t\to\infty} i(t)}{nFDc^*} = \dfrac{\pi^2(a+b)}{\ln[16(b+a)/(b-a)]}$
where $a - b \ll a$ and
b = inner radius of the ring, a = outer radius of the ring

macroelectrodes, with microelectrodes current and electrode surface are not proportional for diffusion-controlled processes; instead current is proportional to the characteristic electrode diameter or radius. Thus, with microelectrodes under diffusion control, the current density is larger the smaller their diameter, whereas with macroelectrodes it is usually independent of surface area.

The time lapse before a stationary state is reached depends both on the size of the electrode and on the diffusion coefficient of the electroactive system. Calculations of Oldham et al.[57] show that for an average diffusion coefficient of $10^{-9}\,m^2s^{-1}$, a 10 μm disk electrode takes approximately 1.3 s and a 1 μm electrode 0.01 s to reach a stationary state, with a deviation $\varepsilon = 5\%$. (According to Equation (12), stationary states can, in theory, also form at macroelectrodes. This would take about 360 h in the case of a 1 cm disk electrode, so that in any event convection influences would dominate.) As it is obvious that several parameters determine the specific properties of such electrodes—the influence exerted by iR will be discussed in Section 2.5—it is very difficult to define an "ultramicroelectrode" in terms of a precise limit for its characteristic dimension. It has become practice to use the term UME for disk electrodes with a diameter smaller than or equal to 20 μm. The term nanode is used for electrodes with a diameter of less than 1 μm.

As expected, the influence of electrode shape is greatest for spherical diffusion fields. The comparison with planar diffusion (Fig. 6) shows that already after 1 s, despite a small

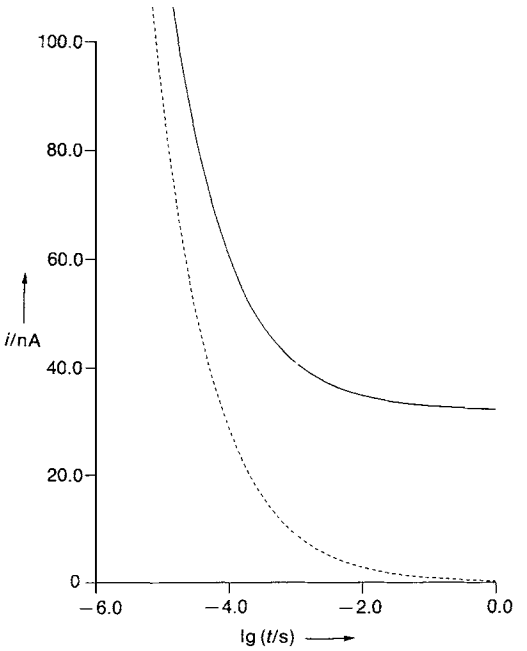

Fig. 6. Simulated current–time curve in chronoamperometry (Cottrell experiment) ($D = 1 \times 10^{-9}\,m^2s^{-1}$, $c^* = 5.4 \times 10^{-2}$ M, $c(0,t) = 0$) for planar (——) and spherical (- - - -) diffusion ($r_0 = 0.5$ μm).

absolute current, the current density at a spherical microelectrode with a diameter of 1 μm is nearly 100 times greater than that at a normal electrode [Eq. (16)].

$$\frac{i_{spher}}{i_{plan}} = 1 + \left(\pi \frac{Dt}{r_0^2}\right)^{1/2} \tag{16}$$

The calculations for cylindrical, band, and ring electrodes prove that these attain only a quasi-stationary state, as the equations for their currents contain time-dependent terms. On the other hand, the current response can be considerably increased by altering band length or ring circumference without changing the diffusion field. This opens interesting perspectives for analytical applications.

2.3. Voltammetry

Whereas in chronoamperometry the potential at the electrode is constant after a single step from the initial to the

final value, in voltammetry the potential changes linearly over time. Starting from an initial potential E_i, a linear potential sweep (potential ramp) is applied to the electrode. After reaching a switching potential E_λ, the sweep is reversed and the potential returns linearly to its initial value,[32, 34] which explains the term *cyclic* voltammetry. The experimental time scale is determined by the potential scan rate (also known as the sweep rate) $v = \Delta E/\Delta t$. This popular electrochemical method was presented in a previous issue of *Angewandte Chemie*.[34]

Ultramicroelectrodes in cyclic voltammetry produce, in principle, the same phenomena as in chronoamperometry. The transition to the stationary state is achieved by reducing the scan rate—and the smaller the characteristic radius of the electrode, the faster the transition. Initially the cyclic voltammograms at "high" v values are wave-shaped; as v declines they become sigmoid polarograms (Fig. 7). As such, they are

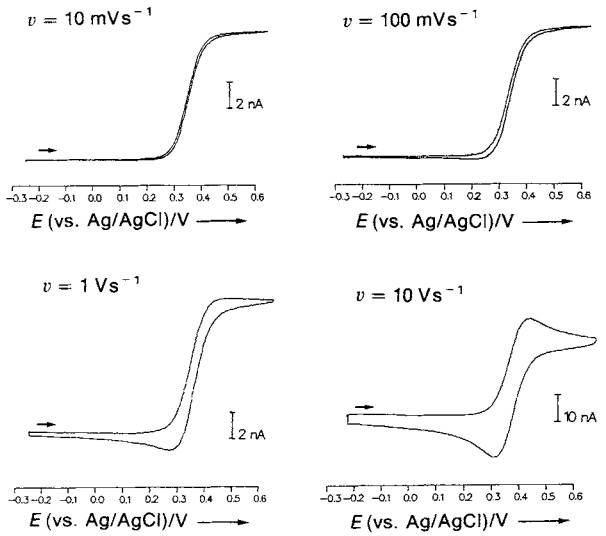

Fig. 7. Experimental cyclic voltammograms of the oxidation of ferrocene ($c = 3.2$ nM) in CH_2Cl_2/0.1 M [TBA]PF_6 (TBA = tetra-*n*-butylammonium) at different scan rates. Measurements taken with a Pt microdisk electrode ($r_0 = 6$ μm).

comparable with the steady-state voltammograms at rotating disk electrodes. This resemblance is due to the formation of stationary (Nernst) diffusion layers, which in the case of rotating electrodes are caused by rapid convectional mass transport, and in the case of microelectrodes are a result of the particular shape of the diffusion field and the high diffusive mass transport rate.

In the stationary state, the currents are time-independent, and the scan rate no longer affects the shape and size of the voltammetric wave. The conditions for the formation of a steady-state differ according to the geometry of the electrodes used. Whereas the diffusion-limited current or the current density corresponds to the values obtained for the stationary state in chronoamperometry (Table 1), theoretical modeling of the entire current–voltage curve has to be done numerically.[60, 61] The only exception is the case of the simple reversible redox process during spherical diffusion to a spherical electrode. For this, Reinmuth[62] has developed a correction formula that can be used to calculate the dimensionless current function $\pi^{\frac{1}{2}}\chi^s(at)$ (which corresponds to a normalized current—s stands for spherical) from the known current function $\pi^{\frac{1}{2}}\chi^p(at)$ (p stands for planar) for planar diffusion [Eq. (17), where σ is the sphericity (17b) and Φ the spherical correction factor (17c)]. The factor a is the normal-

$$\pi^{1/2}\chi^s(at) = \pi^{1/2}\chi^p(at) + \sigma\Phi(at) \tag{17a}$$

$$\sigma = \sqrt{\frac{D}{ar_0^2}} \tag{17b}$$

$$\Phi = \frac{1 - e^{-at}}{1 + e^{\eta - \eta^{(0)}}} \tag{17c}$$

ized scan rate in cyclic voltammetry (defined as $a = vnF(RT)^{-1}$) and $\eta^{(0)} = E^{(0)}nF(RT)^{-1}$ is a normalized potential. The sphericity σ characterizes the extent of the spherical diffusion. For $\sigma = 0$, the limiting case of normal planar diffusion ($r \to \infty$) characterized by the typical transient voltammogram is observed, whereas from $\sigma > 1$ the stationary state ensues (Fig. 8). The transition to the stationary

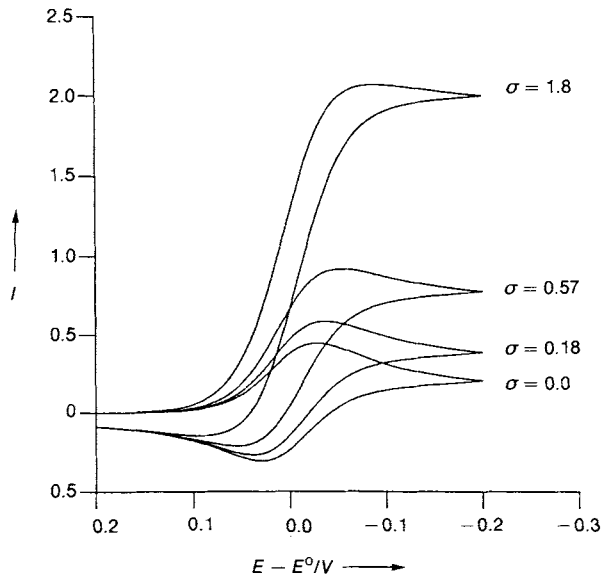

Fig. 8. Simulated cyclic voltammetric diagrams for spherical electrodes with different sphericities. The ordinate gives the current function $\pi^{\frac{1}{2}}\chi(at)$ (= normalized current i) [8].

state takes place at somewhat higher σ values for other electrode geometries.

Larger σ values, usually a consequence of smaller electrode radii, imply higher transport coefficients m (Eq. 11) and therefore higher current densities. A comparison with rotating electrodes (RDE) reveals that the transport coefficient of a spherical electrode with a diameter of 10 μm corresponds to a speed of 10000 rpm. Whereas this is the maximum speed for rotating electrodes, the dimensions of ultramicroelectrodes can be considerably smaller.

One property that distinguishes ultramicroelectrodes from stationary electrodes of conventional size is the increase in the transport rate of the electroactive particles as the electrode radius decreases. The high transport rates mean that with very small electrodes this process can take place as fast or even faster than heterogeneous charge transfer; that is,

instead of being diffusion-controlled, the process becomes kinetically controlled. Unlike the diffusion-controlled case, which is in thermodynamic (Nernst) equilibrium at the electrode, the corresponding stationary current–voltage curves shift and change their shapes depending on the rate of electron transfer (Fig. 9). Thus, ultramicroelectrodes are very

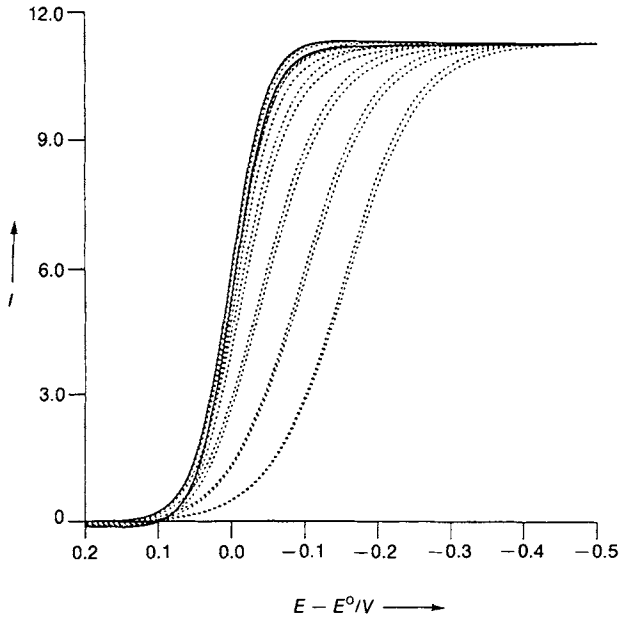

Fig. 9. Steady-state cyclic voltammograms with an ultramicrodisk electrode ($\sigma = 11.1$, ($D = 1 \times 10^{-10} m^2 s^{-1}$, $r = 0.5$ μm, (hemi)spherical diffusion field). k_s^0: (——) > 1, (----) 0.011, 0.0035, 0.0011, 0.00035, 0.00011, 0.000035, 0.000011 ms^{-1}. For $k_s^0 > 1\ ms^{-1}$ and a mass transport coefficient of $m = 0.002\ ms^{-1}$, the electrode process is diffusion-controlled (Nernst case). For $k_s^0 \leq 0.002\ ms^{-1}$, the reaction is kinetically controlled, and the steady-state voltammograms shift with simultaneous minor changes in shape along the potential axis. With the help of theory [63], k_s^0 can be determined from the curves' potential shift.

elegant instruments for determining kinetic parameters of rapid electron transfer reactions. As theoretical considerations show,[63] rapid transfer processes with heterogeneous rate constants of the order of 10^{-2} ms^{-1} can be analyzed by disk electrodes with a diameter of between 5 μm and 0.05 μm. For slower processes, electrodes with significantly larger diameters are adequate. By applying a suitable set of ultramicroelectrodes of different sizes to obtain steady-state voltammograms, one can determine the kinetic parameters of the heterogeneous charge transfer (the transfer coefficient α and the transfer rate k_s^0) as well as the thermodynamic standard redox potential.[63, 64]

There is also another reason why ultramicroelectrodes can accurately determine standard redox potentials. As a result of the high transport rates, the homogeneous chemical processes associated with the heterogeneous charge transfer in the experimental time scale—the latter expressed by the σ value [Eq. (17b)] or the mass transport coefficient m [Eq. (11)]—take place only partially or not at all (Fig. 10). Because the diffusion rates rise with decreasing electrode radius while the rates of homogeneous chemical processes do not change, the effect of diffusion rates on the shape and position of the voltammetric current–voltage curves decreases continuously. Provided that the heterogeneous

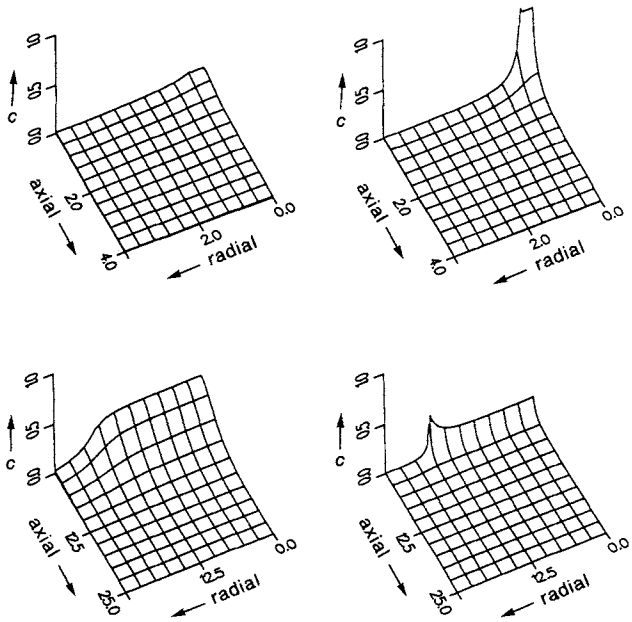

Fig. 10. Two-dimensional concentration profiles for an electron transfer reaction ($R \rightarrow R^-$), to which an irreversible dimerization is coupled ($2R^- \rightarrow R_2^{2-}$, EC_{2irr}, $k_f c/a = 20.0$). Top: microdisk electrode, $\sigma = 5.0$, for the dimer (left) and the anion (right); bottom: macrodisk electrode, $\sigma = 0.1$, for the dimer (left) and the anion (right). The formation of the dimer close to the macroelectrode is very clear; in the case of the microelectrode, the concentration profile of the first anion formed predominates.

charge transfer is very fast, appropriately small electrodes enable the direct determination of the formal redox potential of an electrode reaction by measurement of the half-wave potential $E_{\frac{1}{2}}$.[64] As shall be seen in Section 3.1.1, the relationship between diffusion rate, on one hand, and the reaction rate of the associated chemical reactions, on the other, can be applied to quantitative analysis of the kinetics of such chemical processes.

2.4. The Influence of the Capacitive Current

As with all dynamic electrochemical experiments, chronoamperometry and cyclic voltammetry have to take account of the faradaic current as well as the capacitive current i_c that flows along the electrode when the electrical double layer is charged. The simplest way of simulating the capacitive current is by applying an electrical equivalent circuit, with a resistance that corresponds to the resistance of the solution R_u and a capacitance in series that corresponds to the double layer capacitance C_d. For a single potential step ΔE, i_c (in A) is given by Equation (18), which shows that

$$i_c = \frac{\Delta E}{R_u} \exp\left(-\frac{t}{R_u C_d}\right) \tag{18}$$

the capacitive charging current falls exponentially over time. The smaller the corresponding time constant for charging the double layer (contained in the term RC), the faster the process. According to the expression (19), the drop-off time

$$R_u C_d \sim r_0 \tag{19}$$

for the charging current for ultramicroelectrodes becomes extremely short; they, therefore, hold great potential for measurements in very small time domains.

Because of continual potential sweep, the capacitive current in cyclic voltammetry has two components, one transient, the other steady-state [Eq. (20)]. As the latter predominates at medium and low scan rates, as a rule (20) simplifies to (21).

$$i_c = \left[\left(\frac{E_a}{R_u} - vC_d\right)\exp\left(-\frac{t}{R_uC_d}\right)\right] + vC_d \tag{20}$$

$$i_c = vC_d \tag{21}$$

The capacitive current component i_c disturbs studies on electrochemically induced electron transfer reactions (the faradaic processes), because voltammetric measurements always give the sum of both currents. The capacitive current increases linearly with the scan rate v, whereas the faradaic current i_f changes at $v^{\frac{1}{2}}$. Moreover, when the concentrations of the active redox system are low ($< 10^{-5}$ M), i_f and i_c cannot be adequately separated. Although there is some capacitive effect when ultramicroelectrodes are used in the stationary state, the current ratio i_f/i_c improves drastically as the faradaic component of the current density increases with r_0^{-1}, whereas the capacitive component is independent of the radius. The relationship (22) holds either exactly or approximately for most geometric shapes.

$$\frac{i_F}{i_c} \approx \frac{1}{r_0C_dv} \tag{22}$$

The smaller the characteristic dimension of the electrode and the lower the scan rate, the better the current ratio i_f/i_c in the stationary state of a voltammetric measurement.

2.5. The Ohmic *iR* Drop

As a consequence of the ohmic resistance in an electrolyte, in every electrochemical experiment involving current flow, any prescribed (time-dependent) potential $E_a(t)$ (in V) will be incorrect because of an ohmic potential drop [Eq. (23)]. The

$$E_{eff}(t) = E_a(t) - iR_u \tag{23}$$

lower the conductivity of the electrolyte system and the larger the total current, the larger this effect will be. This influence is particularly conspicuous when the faradaic current is accompanied by a strong capacitive component, as observed, for instance, at high scan rates in cyclic voltammetry (Fig. 11). Moreover, as the combination of R and C_d acts as a low pass filter on the current response (its properties are given by the time constant RC_d), sudden changes in current are more or less strongly distorted.[64b, 65] Because of all these effects, current and potential are mutually dependent in voltammetric analysis, and instead of the set potential scan rate v, an effective rate v' is operative [Eq. (24), Fig. 12].

$$E_{eff}(t) = E_{start} - v't + R_u(C_dv' + i_f) \tag{24}$$

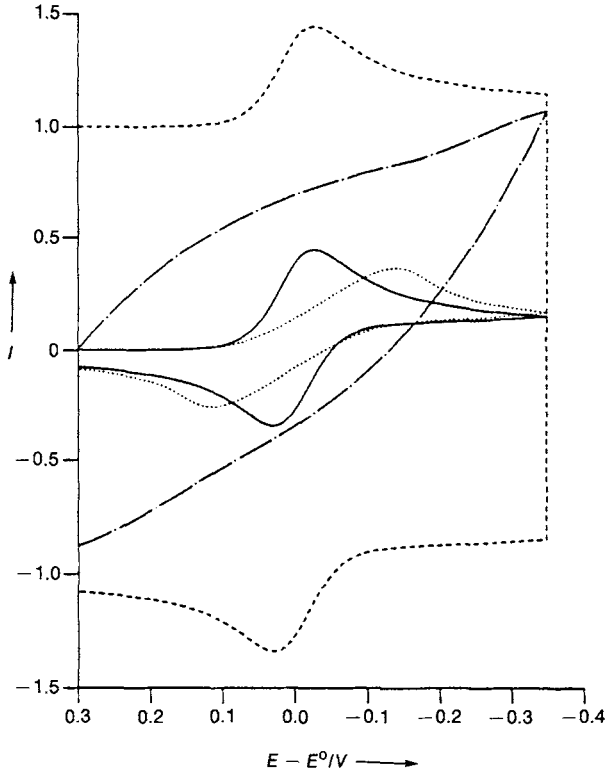

Fig. 11. Simulated cyclic voltammogram for a reversible charge transfer with planar diffusion (——). Presence of a normalized capacitance [65] $\gamma = 1$ (– – –), of a normalized uncompensated solution resistance $\rho = 10$ (· · · ·), and of a combination of these properties (—·—·—) [80b].

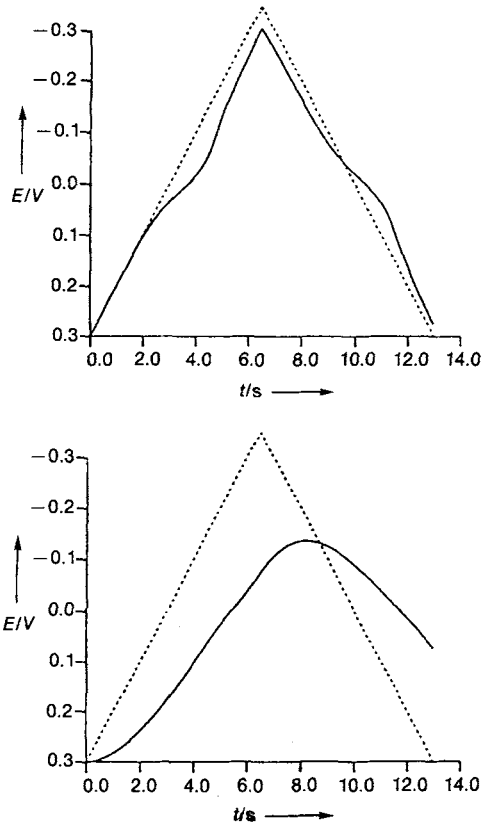

Fig. 12. Potential–time curves for the cyclic voltammograms in Figure 11; measured (effective) potential (——), applied potential (· · · ·). Top: only resistance $\rho = 10$; bottom: resistance $\rho = 10$ and capacitance $\gamma = 1$ [65].

Hence, even in electrolytic solutions with high conductivity, the maximum scan rate for ordinary electrodes with a radius greater than 1 mm is approximately 400 Vs^{-1}.[2, 32] In solutions with low conductivity, this value falls drastically. For example, in benzene the current–voltage curves measured at scan rates of less than 0.1 Vs^{-1} are so distorted that they cannot be interpreted, even though the time constant is negligible, and the only effect is the ohmic potential drop.

In the past one attempted to reduce the iR drop by improving equipment, usually by including a potentiostat in combination with a three-electrode configuration.[32, 66] Through the potentiostat, a reference electrode with high impedance provided a correction signal large enough to compensate for most of the loss of potential at the working electrode. The remaining uncompensated solution resistance was further reduced by electronic feedback,[67] which resulted in possible scan rates of greater than 1000 Vs^{-1} for systems with high conductivity electrolytes and conventional electrodes.

Using ultramicroelectrodes reduces the iR drop so much that it is possible to interpret the results of measurements taken even in extremely diminished electrolytic solutions. Several limiting cases must be distinguished, depending on the experimental conditions. Theoretical[68] and experimental[69] studies show that in the stationary state with a diffusion-controlled limiting current, the ohmic potential drop is no longer dependent on the size and geometry of the microelectrode, but solely on the properties of the electrolyte [Eq. (25), $\varkappa$ = conductivity of the electrolyte system].

$$iR = nFc^{*}D\varkappa^{-1} \tag{25}$$

The iR drop in the case of a low conductivity electrolyte ($\varkappa = 10^{-2}\,Sm^{-1}$, $D = 10^{-9}\,m^2s^{-1}$, $c^{*} = 0.1\,mol\,m^{-3} = 10^{-4}$ M, concentration of an electroactive system) is, according to Equation (25), then 1 mV.

The situation becomes more complicated when the level of the conducting electrolyte in the solution is reduced, for then, in addition to the diffusive mass transport, migration effects can also play a role.[70] As Oldham's calculations and experiments show,[36, 71] the quantitative ratio of conducting electrolyte to electroactive substance can fall to 1:1 without any significant distortion of the current–voltage curve in the stationary state. One reason for this is that the charge transfer at the solution/metal interface raises the ionic density immediately in front of the electrode, which improves the local conductivity $\varkappa$.

The relationship (26) is valid for purely planar diffusion, as exists in the case of high scan rates. Accordingly, as electrode size decreases, so does the ohmic potential drop. As, according to Equation (19), the time constant of the cell decreases parallel to iR, the smaller the radius of the ultramicroelectrode, the more suitable it is for measurements at high scan rates.

$$iR \sim r_0 \tag{26}$$

3. Applications of Ultramicroelectrodes

3.1. Reaction Mechanisms

3.1.1. *Voltammetry under Steady-State Conditions*

As shown in Section 2.3, the magnitude of the diffusion-limited current depends not only on the simple charge transfer, but on whether chemical reactions also take place, possibly coupled with further charge transfer steps. If one uses "large" UMEs ($r_0 < 100$ μm) for the analysis of a three-step reaction[34] comprising one charge transfer followed by a chemical step and subsequently a second charge transfer (ECE reaction), the diffusion-limited current as a rule corresponds to the transfer of two electrons. With smaller microelectrodes, the rate of the chemical step decreases relative to that of the diffusive mass transport (Fig. 10). As a result, the time scale used in steady-state voltammetry is too short for the overall reaction, and therefore n_{app}, the number of electrons measured by the limiting current, gradually declines to 1. This change in the current as a function of the electrode radius can be used to determine the rate constant and the activation parameters of chemical steps in reactions of this nature.[64, 72, 73]

The stationary limiting current's dependence on electrode size can also be used to determine the rate constants of the chemical step in the catalytic EC′ mechanism,[73–77] in which the starting species is regenerated in a chemical step after the heterogeneous charge transfer, and of the reactions preceding the charge transfer. By contrast, in pure EC mechanisms —only a chemical step after the charge transfer—the limiting current is independent of the rate of the next step. Information on the kinetics can only be obtained from the shifts of steady-state voltammograms as a function of the electrode radius.[73]

The use of microelectrodes in steady-state voltammetry to determine rate constants of homogeneous processes has been described several times.[64, 72, 74–79] This method has the advantage that by measuring the diffusion-limited currents with a set of microelectrodes of varying size, the rate constant of a chemical step can quickly be determined. However, this assumes that the precise relationship between the characteristic electrode radius and the kinetics is known, which was as yet only partly the case.

Apart from the catalytic EC′ mechanism,[75–78] the classical ECE mechanism has also been studied in detail. A typical example is the dimerization of triphenylamine (TPA)[80, 81] after its radical cation formation. Under the given experimental conditions ($E_1^0 > E_2^0, E_3^0$), the product tetraphenylbenzidine (TPB) is oxidized to its dication. Overall, a two-electron transfer has apparently taken place [Eq. (27)].

$$2\,TPA \xrightarrow{E_1^0} TPB^{2+} + 2e^{-} + 2H^{+} \tag{27}$$

Figure 13 shows the change in the number of electrons n_{app} at an 8 μm disk electrode as a function of the concentration of TPA. Because the dimerization is a second-order reaction, the rate of the coupling step, and thus the number of electrons transferred, decreases as the concentration of TPA diminishes. A comparison between the experimental data and computer simulations[80] gave a rate constant of

$2.2 \times 10^3\ M^{-1} s^{-1}$, which is in very close agreement with values in the literature.[81] There was some difficulty in interpreting the finding that, in high concentrations of TPA, measurements at microdisk electrodes give rate constants greater than $10^4\ M^{-1} s^{-1}$ on account of the significantly higher n_{app} values (Fig. 13).[72] However, the results did not support the

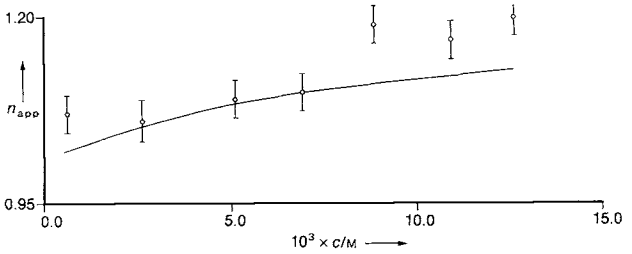

Fig. 13. Numbers of electrons transferred (n_{app}) for the oxidation of triphenylamine for different concentrations in CH_2Cl_2/0.1 M [TBA]PF_6. Experimental points (o) and simulated curve (——). Diffusion-controlled limiting currents measured at a Pt microdisk electrode with diameter 8 μm.

initial assumption that the changes in current density at a microdisk electrode, obtained using a spherical diffusion model with uniform current density over the entire electrode surface, would be false.[72] Rather, it turns out that TPA electropolymerizes to a conducting polymer at a microelectrode[64] (Fig. 14).

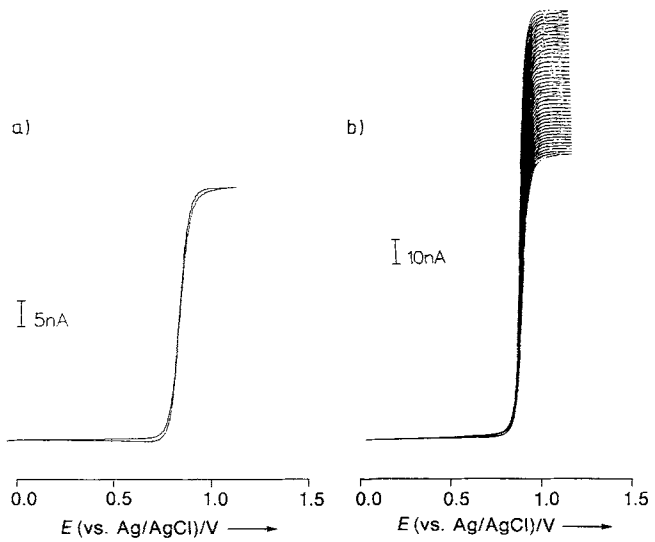

Fig. 14. Experimental steady-state voltammograms for the oxidation of triphenylamine. a) $c = 2.3 \times 10^{-3}$ M, b) $c = 1.2 \times 10^{-2}$ M in CH_2Cl_2/0.1 M [TBA]PF_6, measured at an 8 μm microdisk electrode. The rise in the current in b) is due to electropolymerization effects.

The mechanisms of a whole series of processes used in industrial electrosynthesis have been analyzed.[82] The chief advantage of microelectrodes is the absence of *iR* distortion in the current–voltage curves, even in extremely high concentrations of the reactants, which, of course, enables kinetic and thermodynamic data to be accurately evaluated. For instance, steady-state measurements revealed the experimental conditions under which hydrodimerization of acrylonitrile to adiponitrile (Monsanto process) dominates over the simple reduction of acrylonitrile to propionitrile.[83] Other examples include the catalytic mechanism to methoxylize furane by indirect anodic oxidation in the presence of bromide and methanol[84] and the reductive hydrodimerization of formaldehyde to ethyleneglycol.[85]

Finally, reports on microelectrodes with modified surfaces include studies on electrocatalytic effects of simple redox systems[86] as well as charging processes at conducting polymers or their formation mechanisms.[87, 88] Microelectrodes can also be used in the analysis of slow homogeneous chemical reactions of redoxactive compounds in a reactor to determine the rate constants of the chemical step directly from the time-dependent changes in the diffusion limited currents.[89]

As pointed out above, as the mass transport coefficients *m* increase (that is, as the electrode radius decreases), the diffusion rate may exceed the rate of the associated heterogeneous charge transfer. This makes it possible to determine the rate constants directly from the shift and change in slope in steady-state voltammograms relative to the reversible case.[63] Steady improvements in the construction of ultramicroelectrodes have reduced their characteristic dimensions.[30a, 36, 58a, 90, 91] There have already been reports of microelectrodes with radii of 1–100 nm.[92–94] Hence, theoretically, it should be possible to determine standard rate constants k_s^0 smaller than 1 ms^{-1}. Recent results published by Penner et al.[94] appear to confirm this. Using nanodes ($r_0 = 1-2$ nm), they measured a series of outer-sphere redox couples, for example, $[Ru(NH_3)_6]^{2+/3+}$ (H_2O, 0.5 M KCl) and ferrocene ($Fc^{0/+}$)(CH_3CN, 0.3 M [nBu$_4$N]ClO_4), and obtained k_s^0 values of 0.79 ± 0.44 ms^{-1} and 2.2 ± 1.2 ms^{-1}. Somewhat earlier studies by Bond et al.[95] on ferrocene with 0.3 and 0.5 μm Pt electrodes also produced an unusually high k_s^0 value of 0.064 ms^{-1}. Such high standard rate constants could not be measured in the past. These new results compare surprisingly well with the values predicted by the electron transfer theory of Marcus.[96] Hitherto, standard rate constants of charge transfers obtained with conventional electrodes had produced much lower values, which had raised doubts about the reliability of the theoretical predictions. Apparently, the high transport rates hinder the formation of passivating films, which would otherwise retard the charge transfers in proportion to their thickness and electrode coverage. On the other hand, Penner's results have drawn a lot of criticism. Baranski[97] has shown that relatively large electrodes that are in contact with the electrolyte (through a hollow lagoon left by imperfect fusing and subsequently filled with solution) produce current–voltage curves that are almost identical to those obtained with nanodes. In these circumstances, the theoretical predictions for nanodes are certainly no longer valid; thus the postulated high rate constants have not been unequivocally substantiated.

3.1.2. *Voltammetry with High Scan Rates*

On gradually raising the scan rate when the steady state of an ultramicroelectrode has already been established, one observes the transfer to the semi-infinite planar diffusion as a change from a sigmoid voltammogram to the classic cyclic voltammogram with potential-separated anodic and cathod-

ic waves. These so-called edge effects first drew electrochemists' attention to the peculiar properties of microelectrodes.[6, 13, 19, 55, 98, 99] When microelectrodes with radii between 25 and 500 μm are used, the influence of these edge effects is noticeable at upper scan rates of 5 and 0.05 Vs^{-1}, respectively. Thus, the quantitative data on the kinetics of the heterogeneous charge transfer in these time domains must take into consideration the influence of these edge effects on the peak separation and the shape of the voltammogram.[19, 100–102] On the other hand, in this time scale the iR drop and the capacitance C_d will have little effect on the voltammetric signal. Therefore, using a single microelectrode and varying the scan rate can provide very reliable data on the rate constants of the heterogeneous charge transfer, as described by Nicholson and Shain.[8, 103]

The qualitative jump that makes ultramicroelectrodes so interesting takes effect at scan rates above, say, 500 Vs^{-1}. From about this level the growing iR drop as well as the increasing influence of the RC time constant normally render data obtained with conventional electrodes impossible to interpret. For rates greater than 500 Vs^{-1}, however, conditions for planar diffusion are more or less fulfilled, even for nanodes with radii as small as 1 μm ($\sigma \leq 0.2$). Thus, as v increases, the faradaic current i_f increases proportional to $v^{\frac{1}{2}}$ and the capacitive charging current i_c proportional to v. However, due to the reduction in the radius and the corresponding lower current values, both the RC term [Eq. (19)] and the iR drop [Eq. (24)] decline, and as a result UMEs can be used in a fast-scan range up to 10^5–10^6 Vs^{-1}. "Classical" cyclic voltammetry reaches its limits at scan rates of a few megavolts per second, because the diffusion layer and the electrical double layer then assume almost the same size and can no longer be separated, as theory requires.[104]

In principle, the fast-scan technique provides much the same kind of information as conventional cyclic voltammetry,[34] with one important distinction: the time scale for measurements extends to below 1 μs (for example, at 10^6 Vs^{-1} $\tau = 25$ ns where $\tau = RT/vF$). Thus, it has become possible to measure the redox potentials of highly reactive intermediates[106–108] and rate constants for the rapid heterogeneous charge transfer,[38, 106, 109] as well as to analyze complex mechanisms including chemical steps.[64, 110, 111] Quantitative evaluations of the diffusion-controlled steps of second-order reactions are now also reality. Nor is there any difficulty in investigating and evaluating simple EC reactions.[112]

The group of McCreery were the first to obtain small time constants using ultramicroelectrodes.[113] They were able to prove through chronoamperometry and spectroelectrochemical techniques that within 150 ns concentration profiles of electroactive particles build up in the diffusion-layer region of microelectrodes. With time-dependent absorption measurements of chronoamperometrically produced radical cations of chlorpromazine (CPZ) in the presence of equimolar quantities of dopamine, they obtained values of 6.2×10^7 $M^{-1}s^{-1}$ for the rate constant of the homogeneous $CPZ^{\cdot+}$ cation reduction by dopamine at pH 6.8.

Since then, many voltammetric investigations have been carried out on electron transfer systems with coupled chemical reactions, such as addition,[106, 114] isomerization,[115] dimerization,[116] and homolytic cleavage,[112, 117] to name some examples.

In some cases, the fast-scan technique has made it possible to obtain direct evidence of the existence of reactive intermediates as well as new, unequivocal findings on reaction mechanisms. For instance, in the very rapid homolytic cleavage of halide ions from radical anions of aryl halides, it was not always clear whether the bond-breaking step occurred concurrently with the charge transfer as an inner sphere reaction,[118] or whether the cleavage took place after the formation of the radical anion, that is, in a two-step reaction. Measurements by Saveant et al.[117] of the reduction of 9-bromoanthracene confirm that at scan rates above 100000 Vs^{-1} the formation of the radial anion is reversible. This proves the intermediacy of a highly reactive anion; the rate constant for the subsequent cleavage of the bromide ion is $k_f = 5.9 \times 10^6$ s^{-1}.

For a long time it was disputed whether the cation in the dimerization of radical cations of aromatic amines and heterocyclic compounds first coupled with its neutral species (RS dimerization) or immediately underwent radical cation coupling (RR coupling). Several independent studies support the assumption of RR coupling reactions in most cases.[116] The electropolymerization of heterocycles such as pyrrole and thiophene also involve dimerization steps. Again, Saveant et al. have demonstrated the existence of highly reactive cations of pyrrole and some derivatives within the voltammetric time scale[119] and determined the associated redox potentials. Pyrrole dimerization ($c = 4$ mM) becomes partially reversible at scan rates greater than 18000 Vs^{-1}, which corresponds to an average cation lifetime of 30 μs. The oxidation of 3,3′-dimethoxy-2,2′-bithiophene[120] demonstrates the complexity of the reaction path involving coupling steps in a growing polymer chain. Fast-scan experiments show that the cations formed at the electrode with a rate constant of 10^{+5} initially couple to form a tetramer, which, in turn, after the loss of two protons, also transforms into a dication (Fig. 15). At scan rates greater than or equal to 5000 Vs^{-1} ($c = 1$ mM) the reaction at the electrode is chemically reversible. Further measurements at high concentrations and slow scan rates confirm that the dications comproportionate in solution with unchanged starting monomer, thereby autocatalytically initiating a new coupling step.

The fast-scan technique has proved particularly successful in investigating the kinetics of fast heterogeneous charge transfer reactions.[106, 109, 121–127] Even C_{60}, only recently accessible in large quantities, has already been measured.[114, 127] Provided that the iR influence is reduced to a negligible minimum, the method of Nicholson and Shain[8, 103] can be used without any complications to obtain rate constants from the separation of the peak potentials of the anodic and cathodic waves ($\Delta E_p = E_{pa} - E_{pc}$) (Fig. 16). To determine values between 0.01 and 0.1 ms^{-1}, scan rates must lie between 1000 and 50000 Vs^{-1}. Independently of one another, several groups have established that anthracene, a particularly well-studied compound with a low reorganization energy during charging, has a k_s^0 value of about 0.035 ms^{-1}.[38, 109, 120, 121, 128] Similarly high values were obtained for the ferrocene/ferrocinium redox couple. It

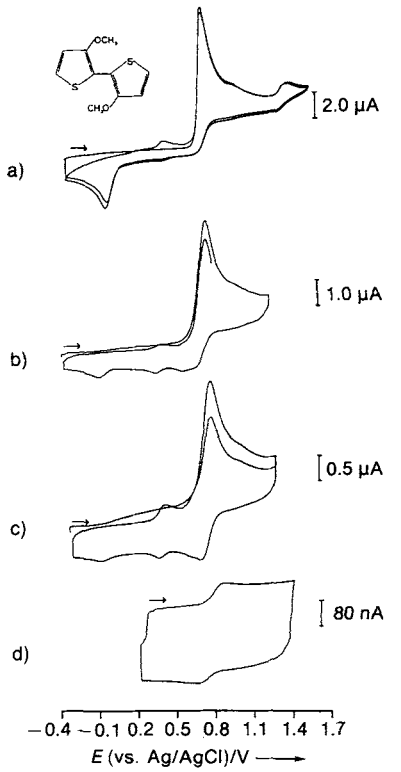

Fig. 15. Experimental cyclic voltammograms for the oxidation of 3,3'-dimethoxy-2,2'-bithiophene in acetonitrile/0.1 M [TBA]PF_6: a) $c = 2 \times 10^{-3}$ M, $v = 100$ mVs^{-1}, $r_0 = 500$ μm; in the reverse sweep the reduction of the cleaved protons is visible at 0.0 V; b) $c = 3 \times 10^{-3}$ M, $v = 20$ Vs^{-1}, $r_0 = 100$ μm; in the reverse sweep the reduction signals of the di- and monocations of the tetramer are also visible; c) $c = 3 \times 10^{-3}$ M, $v = 100$ Vs^{-1}, $r_0 = 100$ μm; d) $c = 3 \times 10^{-3}$ M, $v = 5000$ Vs^{-1}, $r_0 = 2.5$ μm.

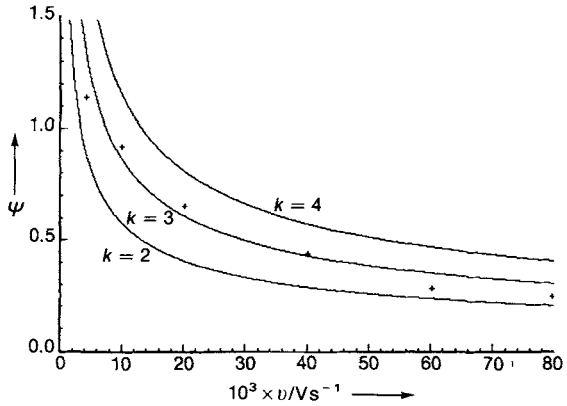

Fig. 16. Experimental and calculated data of the dimensionless ψ parameter as a function of the scan rate [34, 103]. Fast-scan experiments of the reduction of anthracene provided the experimental ψ values from ΔE_p values at different scan rates according to the equation $\psi = f(\Delta E_p)$. The calculation of the ψ values assumes that $k_s^0 = 0.02$, 0.03, or 0.04 ms^{-1}, and $D = 1 \times 10^{-9}$ m^2s^{-1}.

is noticeable that this technique provides much higher rate constants than conventional techniques. This supports the assumption that, as in the steady-state experiments, no passivation occurs at the electrode surface.

At present, the fast scan rather than the steady state technique is preferred for studying reaction mechanisms and measuring kinetic parameters of homogeneous and heterogeneous electrochemical processes. Its crucial advantage is that all methods of evaluation used in classical cyclic voltammetry, including simulation, can be applied. Thus, all the usual mechanisms can be analyzed, and scan rates up to 10^5 Vs^{-1} are accessible even with relatively large electrodes with radii of up to 2.5 μm (Fig. 17). This requires that, apart

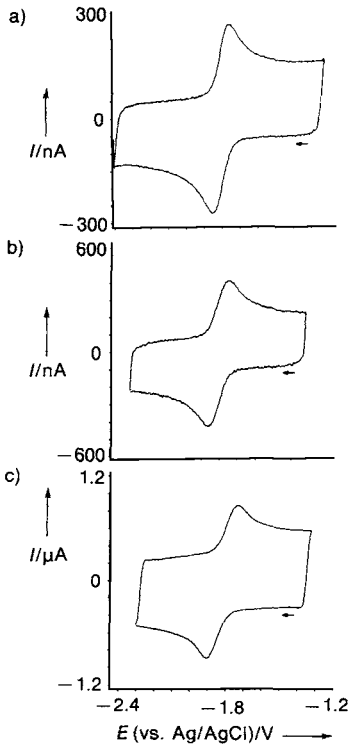

Fig. 17. Fast-scan voltammetry of the reduction of anthracene ($c = 5 \times 10^{-3}$ M) in acetonitrile/0.5 M [TBA]PF_6 at different scan rates. Gold ultramicroelectrode with $r_0 = 2.5$ μm: a) $v = 20\,000$ Vs^{-1}; b) $v = 40\,000$ Vs^{-1}; c) $v = 120\,000$ Vs^{-1}.

from experimental effects due to electrode size and electrolyte resistance, all instrumental influences which might distort the current–voltage curve must be kept as small as possible. Critical features are the construction of the potentiostat, including the current transducer, and the construction of the microelectrode. In respect of the potentiostat and the current transducer, it is very important that amplifiers have an extremely rapid time response and, hence, large band widths are used.[112a, 122, 125] Stray capacitances in the microelectrodes and the cables can cause heavy distortion of the current–voltage curve. For this reason, electrodes with radii of less than 5 μm have to be shielded,[129, 130] and connected to the current transducer and the potentiostat by very short leads. The appropriate iR compensation can produce further improvements.[121, 131]

If very high scan rates of 10^5 to greater than 10^6 Vs^{-1} are used, cell resistance and the time constant will always distort the current–voltage curve. In poorly conducting electrolytes these effects are already apparent at much lower scan rates. It is then better to use simulation to evaluate the data, by inserting the capacitances and resistance values in the Butler–Volmer equation in accordance with Equation 24[60b] (Fig. 18), or by obtaining the real scan rates from the experimental voltammogram and applying them directly in the simulation.[124] Wightman et al.[132] have proposed a method that, given a suitable apparatus, will measure the

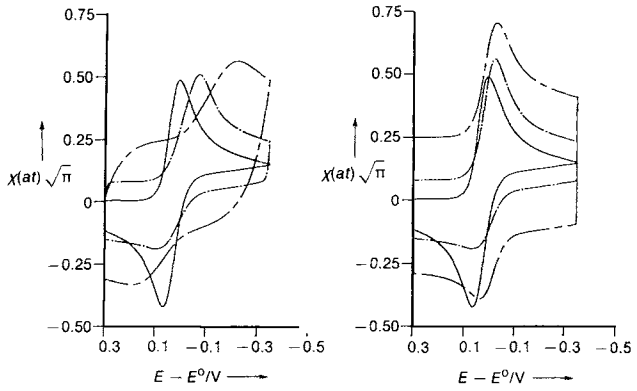

Fig. 18. Simulated cyclic voltammograms for an EC_{2rev} mechanism. Left: with uncompensated resistance $R_u = 41\ \Omega$ and double-layer capacitance $C_d = 1.56\ \mu F$. Right: after correction for the iR drop. Simulation data: $E^0 = 0.0$ V, $D = 1 \times 10^{-9}\ m^2 s^{-1}$, $K_{eq} = 10$, $k_f \times c = 0.1\ s^{-1}$, $k_s^0 = 0.04\ ms^{-1}$; scan rates: (——) $0.1\ Vs^{-1}$, (— · —) $100\ Vs^{-1}$, (— · · —) $1000\ Vs^{-1}$.

background voltammogram without the electroactive system, and then subtract this background current after adding the electroactive sample. However, this technique is only possible if the iR influence is small enough to be neglected.

3.2. Electrochemistry in Poorly Conducting Electrolytic Media

In conventional electrochemical experiments the basic electrolytic solution and the polar solvent ensure high conductivity. Hence, there are no iR problems and consequently no migration effects even at low or medium scan rates. This changes drastically when nonpolar solvents are used, or the concentration of electrolyte is very low, or measurements have to be taken in the solid state or the gas phase. In all these cases the iR drop is very large and cannot be controlled by the usual methods.

As indicated in Section 2.4, the use of UMEs reduces the iR effects, permitting interpretation of voltammetric or amperometric signals even under extremely unfavorable conditions. For example, Bond et al.[36, 133–135] measured the same diffusion-limited currents with 50 μm disk electrodes for the oxidation of ferrocene in electrolyte-free acetonitrile and in electrolytic solution. Moreover, the shape of the steady-state current–voltage curve obtained with electrodes with diameters of less than 1 μm resembles the ideal case of reversible charge transfer very closely. Other authors report similar findings.[136–139] The experimental results agree with Oldham's theoretical predictions[71] that even minute quantities of conducting "impurities" are enough for a sufficiently high conductivity in the immediate vicinity of the electrode. Voltammetric measurements of the oxidation of ferrocene in virtually electrolyte-free acetonitrile with microband electrodes[133] show that the influence of the iR drop depends not on the amplitude of the current response, but mainly on the special flux conditions in the vicinity of the electrode.[68] Despite relatively large currents, the voltammograms show only minor distortions. Some effects have still not been explained. The purpose of measuring in electrolytes with diminished or no conductivity is to obtain electrochemical data under the same conditions as used in spectroscopy or analytical chemistry. Usually, electrolytes have high ionic strengths, imparting significantly different thermodynamic and kinetic properties from those in ideal solutions without added electrolytes. This implies, for example, that in the transition from high to low ionic strengths, ion-pair equilibria, redox potentials, and rate constants of ionic reactions change. Apart from the activity of the involved reactants, the electric properties of the double layer at the electrode also change when the electrolyte concentration is reduced, which renders it difficult to draw unequivocal conclusions from the such experiments. Hence, researchers concentrate on systematically investigating the influence of the concentration of the ground electrolyte on migration and double-layer effects, comparing experimental findings with theoretical predictions, and, finally, determining the limits of electrolytic variations in nonpolar solvents.[70, 71, 134–142] The unexplained phenomena include the frequent appearance of typical cyclic voltammograms in non-electrolytic solutions, despite established steady-state conditions. Presumably the cause lies in changes in solubility after recharging the redox system.

UMEs enable the expansion of the utilizable potential range of aprotic solvents. This is confirmed by measurements in electrolyte-free acetonitrile and SO_2. It could be shown that alkanes are oxidized in acetonitrile[142] at potentials above + 3.5 V, and alkali metal ions were successfully oxidized in liquid SO_2 at potentials[143] of + 5.0 V.

Nonpolar solvents used to be taboo in electrochemical measurements. However, with ultramicroelectrodes the extremely high iR drop falls to tolerable values, and, by choosing suitable electrolytes such as tetrahexylammonium perchlorate ([THA]ClO_4) or $NaBPh_4$–crown ether complexes, amperometric or potentiodynamic experiments in solvents such as benzene, toluene, or even hexane provide interpretable results.[26, 36, 106, 144, 145] The precondition for the success of such experiments is that the electrolytes are soluble enough, and that they dissociate to some degree to provide an acceptable level of conductivity in the solution. Up to now, the chemistry of redox reactions in hydrocarbons could only be analyzed with spectroscopic methods; now, for the first time, it will be possible to use electrochemical measurements for quantitative studies. The growing interest in electrochemical investigations in aromatic hydrocarbons, alkenes, and alkanes is largely due to the fact that ionic reactions take place at quite different rates in weakly polar solutions and in polar media. Measurements that cover as wide a range of polarity as possible provide precise insights into the relationships between solvation and chemical reactivity, including the kinetics of electron transfer. For example, voltammetric studies[64] on the kinetics of the dimerization of radical anions of 9-cyanoanthracene show that the corresponding rate constants increase by almost four orders of magnitude from 1.4×10^3 to $9.0 \times 10^6\ s^{-1}\,M^{-1}$ between benzene ($\varepsilon = 2.27$) and the extremely polar *N*-methylformamide ($\varepsilon = 190$) (Fig. 19). Experiments of this nature show that particles with the same charge can form a covalent bond at high rates despite coulombic repulsion.

The use of nonpolar solvents also has interesting analytical applications. There is a discussion, for instance, on the use of supercritical CO_2 as a mobile phase in capillary chromatography.[146] Voltammetric measurements in this medi-

um are reproducible only after small quantities of water have been added; the use of ion-conducting membranes improves the results.[147]

Steady-state voltammetry is another challenging field for ultramicroelectrode techniques. However, to ensure that the *iR*-drop component always remains sufficiently small for the use of nanodes, conductivity values may not fall below $10^{-6}\,S\,cm^{-1}$. For this reason, inorganic[148] and organic[149] steady-state electrolytes as well as frozen electrolytic solutions[27, 150] (cryoelectrochemistry) are the most popular areas of research. Because under solid-state conditions, diffusion coefficients lie between 10^{-11} and $10^{-16}\,m^2\,s^{-1}$ ($\sigma \leq 0.3$), that is, orders of magnitude smaller than in solution, instead of steady-state curves, voltammetric measurements at UMEs often reveal a range of conditions from a transition between the steady state and planar diffusion up to classical cyclic voltammetric situation. An additional complication is the appearance, especially at very low temperatures, of voltammetric curves typical of surface processes without diffusive mass transport. Although many details are still unclear, one plausible explanation assumes that liquid microphases survive in solution well below freezing point,[150, 151] adhering to the electrode surface in thin layers.

One field of electrochemistry with spectacular promise is UME applications in the gas phase. Pons and Fleischmann have published several reports on such experiments.[28, 152, 153] It is important that a very narrow insulating field separate the working and the auxiliary electrodes, for example, in a ring–disk arrangement or two half-disks. The conductivity across the insulating gap takes place either by means of a conducting membrane or in the presence of moisture in the form of proton transport.[152a] Microelectrode detectors, affixed for this purpose at the outlet of a gas chromatograph, were able to determine the individual components of a hydrocarbon mixture as well as a heat conducting detector (Fig. 20).

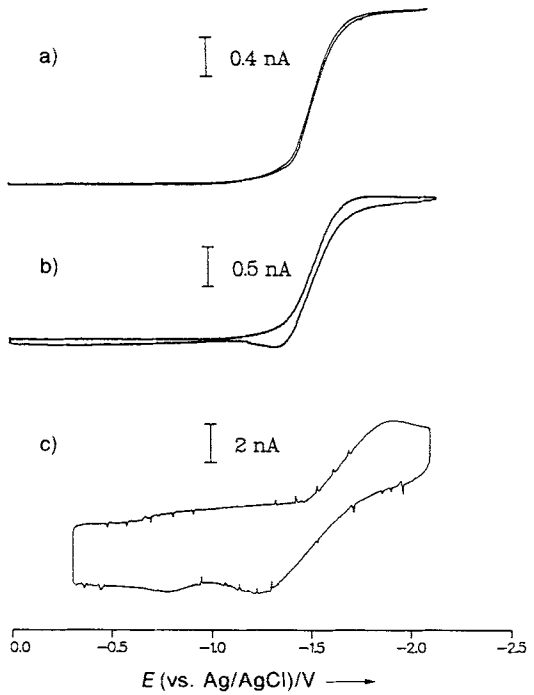

Fig. 19. Cyclic voltammograms for the reduction of 9-cyanoanthracene ($c = 1 \times 10^{-3}$ M) in benzene/0.5 M $[TBA]ClO_4$ at different scan rates: a) $100\,mV\,s^{-1}$, b) $1\,V\,s^{-1}$, c) $100\,V\,s^{-1}$.

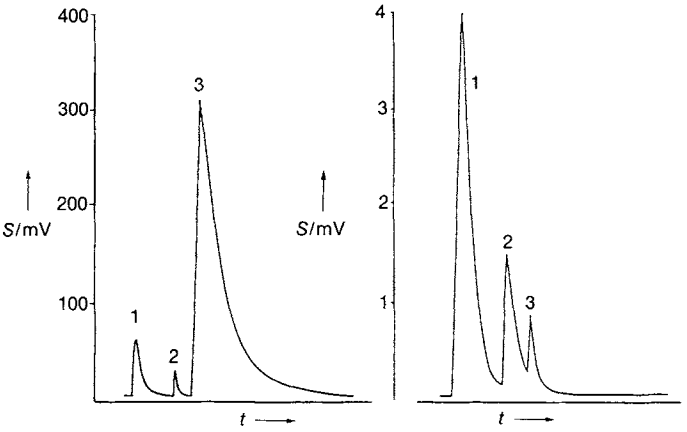

Fig. 20. Response of detectors in gas chromatography for an injection volume of 1 μL of a sample containing 30% toluol (1), 30% *ortho*-xylol (2), and 40% cyclohexanone (3). Injection port 190 °C, column 90 °C, outlet port 120 °C. Left: palladium microelectrode (potential + 3.0 V); right: thermal-conductivity detector. S = signal strength [152b].

3.3. Exploiting the Smallness of Microelectrodes

As already mentioned in the introduction, UMEs have a cardinal advantage because of their size, which makes it possible to conduct electrochemical measurements in minute volumes and observe discrete spatial events in microscopically small areas. Hence, it is not surprising that microelectrodes were first used for measurements in living systems. A report on electrochemical studies on the partial pressure of oxygen in tissue was published as early as 1938.[23] Baumgärtl and Lübbers' invention of the microcoaxial needle electrode, which, including the reference electrode, was only 0.3 to 0.5 μm at the tip, enabled routine measurements of oxygen gradients in cell tissue as well as at the gas/liquid interface or in pores of polymers.[154] Another important aspect of in vivo voltammetry is tracing neurotransmitters (catecholamines) or their metabolites (ascorbic acid) in the brain or in nerve cells. Building on pioneering work of Adams et al.,[155] improvements in the manufacture of microelectrodes[156–158] as well as technical progress[159, 160] have made it possible to take measurements both in living tissue and in unicellular organisms or single cells.[161] Surface-modified electrodes are becoming increasingly popular as they provide greater selectivity and sensitivity.

The patch-clamp technique,[162] for which Neher and Sakmann recently received the Nobel Prize,[163] also uses "microelectrodes". Whereas the above-mentioned microvoltammetric electrodes can cause and measure redox processes in a cell, the patch-clamp technique employs micropipettes, which measure electric currents that appear when the stimulated cell causes ions to move through channels in the cell membrane. Efforts are now being made to combine the two methods.[164]

A lot of work has been done on the electrocrystallization of metals, metal oxides, and organic salts. But quantitative

descriptions of growth processes in progress were extremely difficult because, statistically, nuclei form at several points on an electrode surface, and the measured current transients would integrate all these events. Naturally, the number of nucleation processes on the minute surface of ultramicroelectrodes is considerably smaller than on macroelectrodes. Therefore, under favorable circumstances it should be possible to detect the individual steps in the formation of a single nucleus and to analyze the kinetics of its growth process[20, 165, 166] (Fig. 21). Measurements obtained with

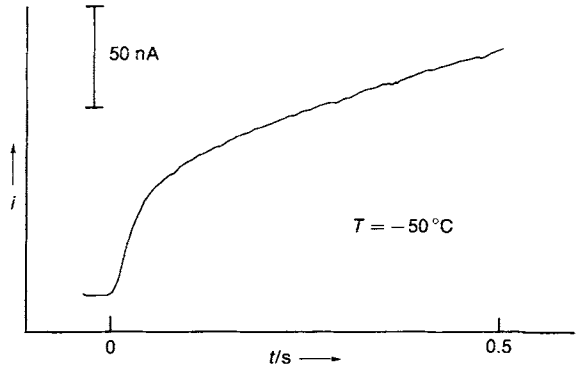

Fig. 21. Potentiostatic current–time transient for the growth of a crystal nucleus of a fluoranthene radical cation salt ($c = 2 \times 10^{-2}$ M) in acetonitrile/0.1 M [TBA]PF_6, measured at an 8 μm Pt disk electrode with a potential of +1.4 V vs. Ag/AgCl.

an ensemble of microelectrodes should provide unequivocal information on the rates of nucleus formation. The relatively large distances between the individual microelectrodes prevents the individual crystal nuclei from colliding with one another as they grow, which would unleash an undesirable dispersion of growth.[166] In recent articles, Oldham et al.[167] discuss the different mechanism of electrochemical mercury precipitation on carbon or metal microelectrodes from a thermodynamic point of view, and show that the type of precipitation process is conditioned by the surface energy at the electrode/electrolyte interface and the relative sizes of all the components involved.

The small size of UMEs is also useful for studying corrosion phenomena. They can be employed as probes to scan corrosive processes in closely defined spaces,[168] on the one hand, and serve as experimental models for local corrosive processes,[169] on the other. The small time constants are another advantage: rapid events can be recorded without complications, and interference from background currents during corrosive processes are kept to a minimum.[170]

A fascinating new development in UME techniques is based on the fact that the faradaic current, which, in the presence of an electroactive substance under diffusion-controlled conditions flows over the "tip" of the ultramicroelectrode, depends on whether the diffusion field of the microelectrode is disturbed by external influences. One consequence is that in the immediate vicinity of an insulating surface the current flowing over the UME is smaller than the undisturbed limiting current (Fig. 22). The extent of the change in current is determined exactly by the distance between the microelectrode and the nonconducting surface. Moreover, the smaller the electrode, the stronger the effect.

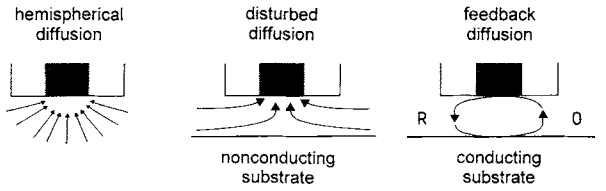

Fig. 22. Typical shapes of diffusion fields in scanning electrochemical microscopy. Left: undisturbed hemispherical diffusion field far from the substrate; diffusion-limited current i_l according to Equation (15). Center: disturbed diffusion field close to a nonconducting surface, $i < i_l$. Right: electroactive starting system regenerated (feedback effect) at a conducting substrate, $i > i_l$ [172b].

Thus, a piezoelectric scanner that moves the tip of the microelectrode parallel to the surface of a structured substrate can monitor the tip current as a function of its position. This setup generates an image of the surface topography of the sample (Fig 23). The recording technique resembles scanning

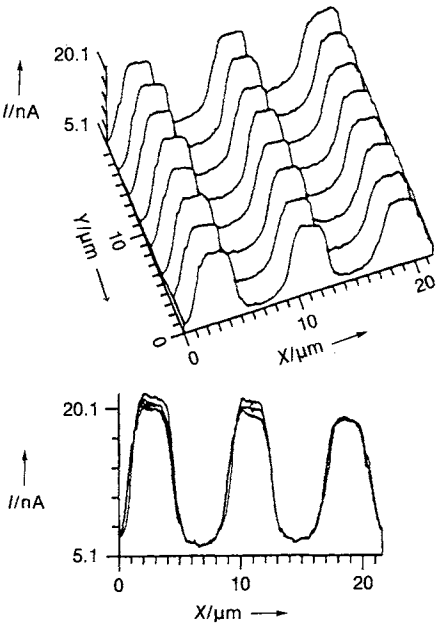

Fig. 23. SECM image of a Pt interdigitated structure on a SiO_2 substrate. Probe: Pt disk electrode embedded in a 0.3 μm poly(methyl methacrylate) layer, disk diameter ~0.5 μm, $E_s = -0.77$ V vs. SCE (saturated calomel electrode); aqueous solution with 40 mM methyl viologen and 2 M KCl. Top: three-dimensional view. Bottom: side view [174b].

tunneling microscopy (STM)[171] as far as the movement of the electrode across the substrate surface under investigation is concerned, but the principles of measurement differ. Whereas in STM a tunnel current flows between the tip of the electrode and the substrate, the current flow in the case described here is based on redox processes that take place at the tip of the electrode or at the substrate surface (see below). Their extent is controlled by the kinetics of the charge transfer at the phase interfaces as well as by the diffusive mass transport. For this reason, this method is known as scanning electrochemical microscopy (SECM). It is a fairly recent development, largely a product of Bard's group.[29, 172] Its resolution is not as high as that of STM, but should, with further improvement, approach the 50 nm limit. In a variant of this technique, the substrate surface itself is conductive,

and thus can be given a different potential than the microelectrode. This allows, for example, a substance R produced by reduction ($O + e \rightarrow R$) at the electrode tip to be reoxidized at the substrate, a feedback which increases the diffusion current at the microelectrode (Fig. 22). This technique has advantages: the insulating shield of the electrode causes less interference than in the direct mode, and the stronger current improves depth resolution.[173] Both methods have been used to study surfaces of interdigitated arrays[174,175] (Fig. 23), polymers,[175,176] and biological samples.[177] Apart from topographical information, the SECM technique provides data on heterogeneities of the charge transfer at different points on a substrate surface.[178,179] This enables one to detect space-dependent changes in the chemical properties of surfaces, including, for instance, biocatalytic activities.[180] Furthermore, varying the perpendicular distance between the microelectrode and the substrate will provide information on diffusion profiles and kinetic parameters of homogeneous reactions.[181] This is achieved by generating different potentials at the substrate electrode and the microelectrode with a bipotentiostat, analogous to the ring–disk electrode.[182] Thus, the particles generated at the substrate can be detected with spatial and temporal resolution at the microelectrode (generator-collector mode[182]). Instead of using the microelectrode as detector, Anson[183] used the substrate electrode. This not only provides greater sensitivity to current and a better current-to-noise ratio; it also allows the two electrodes to be placed farther apart.

Interesting technical applications of SECM in the field of microsystem technologies include electroplating and etching.[184] Using the direct mode, one can generate, for example, thin metal strips in an ionic conducting polymer film, for instance Nafion containing gold, silver, or palladium ions, by polarizing the microelectrode tip to a negative potential and the substrate tip attached to the back of the polymer film to a positive potential. In the feedback mode, a mediator is oxidized or reduced at the microelectrode, which, after oxidative etching or reductive metal deposition at the substrate, is then transported back to the microelectrode, where it undergoes a new redox reaction.[185]

Reports on the SECM principle indicate an enormous range of possibilities for surface analysis, microgalvanization, and microetching. Present efforts to increase the resolution and sensitivity of the technique focus on reducing the size of the microelectrode tip[174b] and improving procedures.[186]

The aforementioned generator–collector principle can also be applied to stationary electrodes by polarizing a series of band electrodes in very close proximity (μm range) at different potentials. Reactive intermediates generated at one electrode, or which emerge in a subsequent chemical step, are detected at the collector electrode.[187] Measuring the current density (collector efficiency) as a function of the distance between the band electrodes and evaluating the findings with the aid of digital simulation provides kinetic and mechanistic information on the system under investigation. Studies of this nature have been carried out on recombination and electrochemical luminescence (ECL) of radical ion pairs, and on the catalytic oxidation of ascorbic acid and aminopyrine by $K_3[Fe(CN)_6]$.[39,188] Not only pairs of band electrodes, but also triple band electrodes[189] and interdigitated array electrodes[190] are now also being used for such work.

3.4. Ultramicroelectrodes in Chemical Analysis

Although analytical problems in the widest sense constitute an important aspect of this article, so far not much has been said about the use of UMEs in analytical chemistry, apart from electrochemical measurements of concentrations in the gas phase.

In principle, all the unconventional properties of ultramicroelectrodes can be exploited with advantage in chemical analysis. High mass transport rates and reduced capacitive effects produce both a marked improvement in the faradaic/capacitive current ratio [i_f/i_c; see Eq. (22)] and a better signal-to-noise ratio, which raises overall system sensitivity.[39,191] Digital and analog filters hold promise of further improvements.[192] The low values of the *RC* time constants lead to a fast drop in the capacitive charging current. As a result, traditional voltammetric pulse methods[32] used in chemical analysis, such as (differential) pulse voltammetry, staircase voltammetry, and square-wave voltammetry, should prove particularly suitable for UME measurements. This has been largely confirmed in experiments, some of which introduce new technical improvements.[133,138c,193–195] By using square-wave voltammetry in conjunction with a hydrodynamic modulation achieved by vibrating a microcylinder, the detection limit for ferrocene in acetonitrile could be lowered to 3×10^{-8} M.[196]

UMEs also have great potential in the stripping methods used in trace-element analysis. Because of the high mass transport coefficients, the solution does not have to be stirred during accumulation, and accumulation proceeds far faster. As the substance being analyzed was concentrated in a very small volume (the microelectrode), it is stripped completely during the anodic scan. This provides very sharp, easily interpretable peaks.[50,197–199]

If the characteristic dimensions of the microelectrodes are less than 10 μm, the high mass transport coefficients will keep the convection and hydrodynamic influences on a microelectrode's current response so small that they can be ignored. This phenomenon can be exploited to great advantage for electrochemical detection in flow systems, for example, in flow injection analysis or high performance liquid chromatography (HPLC).[200–202]

Because the *iR* drop has little influence on the current response, additional electrolytes are unnecessary, and the solution requires minimal conditioning. Furthermore, investigations can be carried out directly in samples, for example in fruit[203] (Fig. 24). Recently, band,[49] cylinder,[204] and array electrodes[133,203,205] have been used for these measurements instead of microdisk electrodes. They make it possible to measure relatively large currents in the lower μA range with the typical advantages of ultramicroelectrodes, which considerably reduces time and effort compared with other analytical techniques. The advantage of array electrodes is that they are easy and cheap to reproduce with modern lithographic techniques (see Section 4), and thus can be discarded after use.[206] Array electrodes also find in-

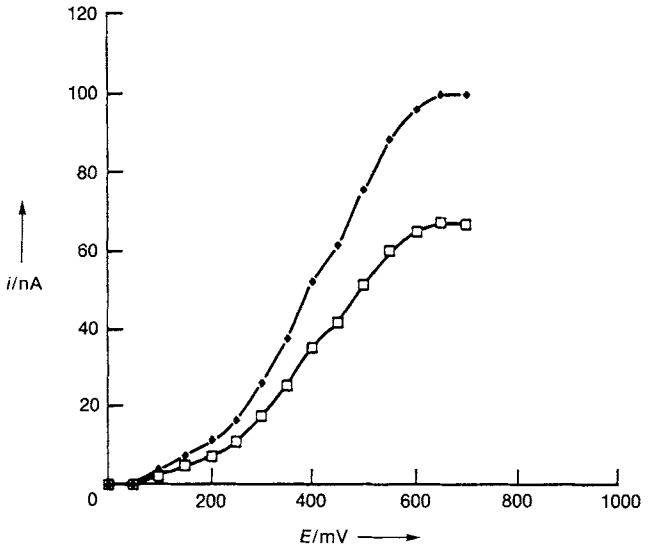

Fig. 24. Steady-state measurements of the oxidation of ascorbic acid in a Granny Smith apple with a gold microband electrode. $v = 20\ mVs^{-1}$: • at the surface, □: in the apple [203].

creasing application in the manufacture of electrochemical chemo- and biosensors, because their combination of small dimensions and relatively large sensitive area reduces response times and the signal-to-noise ratio.[207]

4. Construction of Ultramicroelectrodes

By now it should be clear that the main variables in the use of ultramicroelectrodes are geometry and size. The choice depends on the field of application. In recent years, therefore, many techniques have been developed to produce ultramicroelectrodes in varying geometries, sizes, and materials.

The most important type of electrode is still the disk electrode, which is usually made of platinum, palladium, gold, or carbon and, apart from the disk surface, fused into glass or embedded in plastic to isolate it completely from the electrolytic environment.[6b, 36–38, 63a, 90–94, 125, 132] It is essential that the electrode is reusable. This means that the electrode surface must be easy to clean; details can be found in the literature.[30a, 158] The details of techniques for manufacturing disk electrodes with diameters smaller than 0.6 μm have also been published. Because the electrode material becomes increasingly sensitive to temperature as the diameter decreases, "pullers" are used in the fusion process.[163] This step has been borrowed from the patch-clamp technique, which has long used pullers in the manufacture of extremely thin glass capillaries. They make it possible to set the exact temperatures needed to gradually soften the glass. The perfect seal obtained at the interface between glass and electrode material, a precondition for quantitative investigations with ultramicroelectrodes (Fig. 25), corroborates the quality of these fusion processes. Another problem with electrodes with diameters below 10 μm is the stray capacitances caused by additional capacitance between the electrode wire, the insulating environment, and the electrolytic solution.[129, 208, 209] It can lead to a drastic decline in the faradaic/capacitive current ratio (Figs. 26a and 27a). Recently, shielded electrodes have brought a noticeable improvement in this respect: the electrode capacitance is

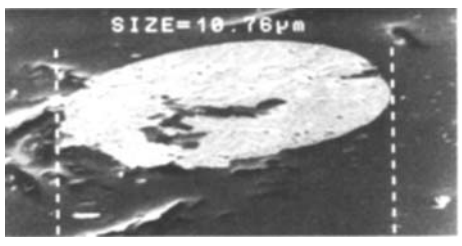

Fig. 25. Electron micrograph of a platinum disk electrode with a diameter of 10 μm embedded in soft glass.

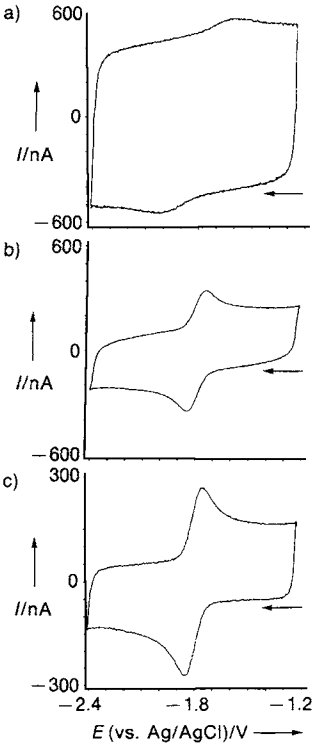

Fig. 26. Fast-scan voltammetry of the reduction of anthracene (5×10^{-3} M) in CH_3CN/0.5 M [TBA]PF_6; $v = 20000\ Vs^{-1}$; measured with a gold ultramicroelectrode with $r_0 = 2.5$ μm; a) without shield, b) shield incorporated but not activated, c) shield incorporated and activated.

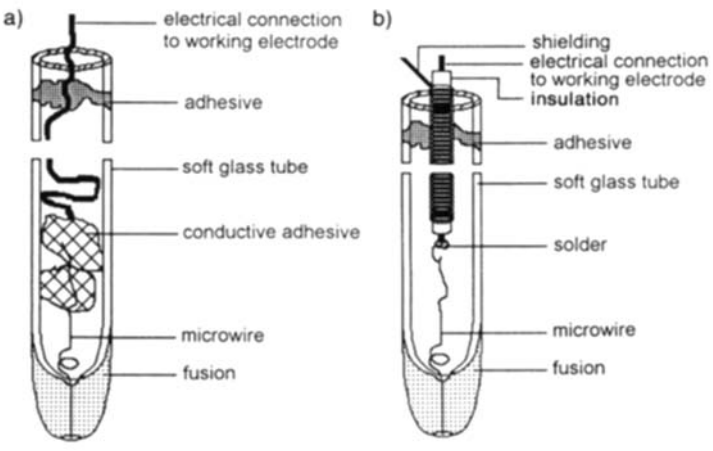

Fig. 27. Schematic setup of microdisk electrodes. a) Conventional electrode without shield. b) Electrode with electric shield.

significantly reduced by incorporating an additional, grounded metal shield or a coaxial cable in the glass fusion[129, 130b, 210] (Figs. 26b,c and 27b).

Whereas a metal wire fused into the glass is virtually indispensable in disk-electrode experiments in aprotic solutions, there is no problem in using carbon fibers as electrode material for studies in aqueous media, especially on biological objects.[30a, 211–215] The carbon fiber tips with characteristic diameters of up to 400 nm are produced by, for example, electrochemical etching or burning in a flame and isolated from the medium by electropolymerization of polyoxyphenylene.[212, 215, 216] The thin polymer layer adheres well and ensures that only the narrow tip retains its conductivity (Figs. 28 and 29). A common problem associated with carbon fiber electrodes is very slow electron transfer, which calls for appropriate activation of the tip.

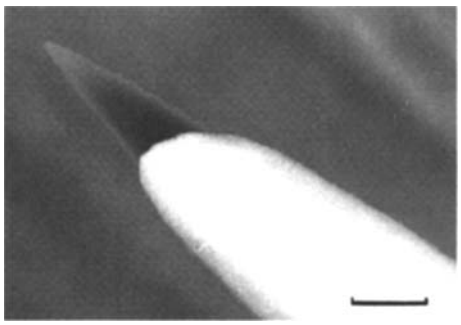

Fig. 28. Electron micrograph of a carbon-fiber tip (pitch fiber P100, Union Carbide), stuck into silicon rubber and then copper-plated. This was an experiment to test the possibility of leaving just a few μm free at the tip of the fiber on the principle of regioselective insulation. To heighten the contrast, Cu was chosen instead of insulating polyoxyphenylene [215]. The bar represents 3 μm.

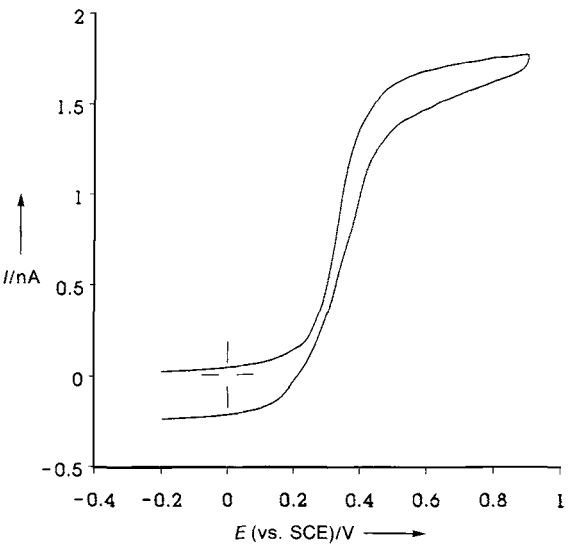

Fig. 29. Steady-state voltammogram of the oxidation of $K_4[Fe(CN)_6]$ ($c = 2$ mM) in H_2O/0.1 M KCl, $v = 1\ Vs^{-1}$, measured with a carbon-fiber tip [215].

Apart from the microdisk, microcylinder,[41, 51] microring,[43, 44] and microband electrodes[39–42] are also used. Band electrodes, employed as single-band electrodes, as double or triple band arrangements, or as arrays, have become increasingly popular in recent years. One reason is that, despite their narrowness, microband electrodes have a relatively large surface, and, therefore, give a favorable signal-to-noise ratio. Band electrodes serve as chromatographic detectors in analytical chemistry, are used to study reaction mechanisms and diffusion processes, and act as devices in microelectronics. There are different ways of manufacturing these electrodes.[217] The classical method is to fuse very thin strips of metal foil between sheets of glass or to embed them in a synthetic material with the aid of epoxy resins or films of Teflon. A far more elegant method, applicable into the lower nm range, consists of evaporation or sputtering of metals onto insulating substrates, which are then covered with a second insulating layer.[38–40, 218–220] Promising developments are microlithographic techniques, which have long been used in the electronic and semiconductor industries.[133, 187, 188, 217, 221–223] The most popular variants in electrode manufacturing are photolithographic techniques, which produce structures as narrow as 0.5 μm.[217]

5. Conclusions

Though the unconventional properties of ultramicroelectrodes were recognized only at the beginning of the 1980s, the exponential growth in literature on the subject testifies to their success. Numerous applications have stimulated the development of new methods and opened up previously inaccessible fields of research to electrochemistry. Present research goals include voltammetric measurements of the thermodynamics and analytical chemistry of poorly conducting electrolytic media from the solid state, through nonelectrolytic solutions, to the gas phase, as well as of the mechanisms and kinetics of very fast electrochemical reactions. With in vivo voltammetry, metabolic processes can be observed in cell tissue without causing any damage, and in the field of applied electrochemistry new strategies for sensor development[207] and corrosion research[224] are emerging. Moreover, with the new SECM technique an electrochemical method is available, which, for the first time, makes it possible to derive images of surface structures by measuring faradaic currents, as well as to microgalvanize and etch surfaces.

The persistent trend to smaller electrodes and simpler manufacturing techniques, assisted by efficient microsystem technologies and advances in laser research,[225] will considerably expand the scope of applications. The many aspects of an electrochemistry in a "natural" environment will surely encourage more intense interdisciplinary cooperation with other fields in chemistry, biology, and the material sciences. The priority status of the fast-scan technique and probably the SECM technique, too, should ensure that they reach a degree of perfection in the near future, which will turn them into routine methods using commercial equipment. The application of the techniques of microelectroplating will soon be used to build elements for microelectronics and micromechanics that will be able to compete with the products of photolithographic techniques. After an extraordinarily successful start, microelectrochemistry has a very promising future.

I am indebted to my excellent co-workers for their commitment and their considerable contributions in the form of ideas and experiments, which have gained for my research group its reputation in the field of ultramicroelectrodes. Their names will be found in the references. Dr. Michael Störzbach's conception of simulation models and his construction and application of UMEs were pioneering developments in this field. To him go my special thanks. I am grateful to the Deutsche Forschungsgemeinschaft, the Volkswagen Foundation, and the Fonds der Chemischen Industrie for the generous support they have given our work. Mr. Danny O'Hare, Imperial College, London, and Dr. Christian Amatore, Ecole Normale Supérieure, Paris, provided many suggestions in numerous discussions, for which I thank them both. Some aspects of the work mentioned in the text were only possible through the cooperation of other groups, in particular the Max-Planck-Institut für Systemphysiologie in Dortmund and the research group of Professor Besenhard, University of Münster. Finally, I wish to thank Dipl.-Chem. Peter Tschuncky, whose work on the fast-scan technique has set new standards for quality in microelectrodes.

Received: February 3, 1993 [A 917 IE]
German version: *Angew. Chem.* **1993**, *105*, 1337
Translated by John Richardson, Freiburg

[1] K. J. Vetter, *Elektrochemische Kinetik*, Springer, Berlin, **1961**.
[2] P. Delahay, *New Instrumental Methods in Electrochemistry*, Interscience, New York, **1954**.
[3] a) J. Heyrovsky, *Chem. Listy* **1992**, *16*, 256; b) J. Heyrovsky, *Recl. Trav. Chim. Pays-Bas* **1925**, *44*, 488.
[4] D. MacGillavry, E. K. Rideal, *Recl. Trav. Chim. Pays-Bas* **1937**, *56*, 1013.
[5] a) H. A. Laitinen, I. M. Kolthoff, *J. Am. Chem. Soc.* **1939**, *61*, 3344; b) H. A. Laitinen, I. M. Kolthoff, *J. Phys. Chem.* **1941**, *45*, 1061.
[6] a) A. J. Bard, *Anal. Chem.* **1962**, *33*, 11; b) P. J. Lingane, *Anal. Chem.* **1964**, *36*, 1723; c) Z. G. Soos, P. J. Lingane, *J. Phys. Chem.* **1964**, *68*, 3821.
[7] a) I. Shain, K. J. Martin, *J. Phys. Chem.* **1961**, *65*, 254; b) I. Shain, K. J. Martin, J. W. Ross, *ibid.* **1961**, *65*, 259.
[8] R. S. Nicholson, I. Shain, *Anal. Chem.* **1964**, *36*, 706.
[9] D. I. Dornfield, D. H. Evans, *J. Electroanal. Chem.* **1968**, *20*, 341.
[10] Y. Saito, *Rev. Polarogr.* **1968**, *15*, 177.
[11] W. Grunewald, *Pfluegers Arch.* **1970**, *320*, 24.
[12] C. R Ito, S. Asokura, K. Nobe, *J. Electrochem. Soc.* **1972**, *119*, 698.
[13] J. B. Flanagan, L. Marcoux, *J. Phys. Chem.* **1973**, *77*, 1051.
[14] R. N. Adams, *Anal. Chem.* **1976**, *48*, 1126A.
[15] R. Lines, V. D. Parker, *Acta Chem. Scand. Ser. B* **1977**, *31*, 369.
[16] B. Speiser, A. Rieker, *Electrochim. Acta* **1978**, *23*, 983.
[17] J.-L. Ponchon, R. Cespuglio, F. Gonon, M. Jouvet, J.-F. Pujol, *Anal. Chem.* **1979**, *51*, 1483.
[18] P. N. Swan, Dissertation, University of Southampton, **1980**.
[19] J. Heinze, *Ber. Bunsenges. Phys. Chem.* **1980**, *84*, 785; *ibid.* **1981**, *85*, 1096.
[20] a) B. R. Scharifker, G. J. Hills, *J. Electroanal. Chem.* **1981**, *130*, 81; b) G. Hills, A. K. Pour, B. Sharifker, *Electrochim Acta* **1983**, *28*, 891.
[21] F. G. Cottrell, *Z. Phys. Chem. Stoechiom. Verwandschaftsl.* **1902**, *42*, 385.
[22] R. M. Wightman, *Anal. Chem.* **1981**, *53*, 1125A.
[23] a) L. R. Blinks, R. K. Skow, *Proc. Natl. Acad. Sci. USA* **1938**, *24*, 420. b) P. W. Davies, F. Brink, *Rev. Sci. Instrum.* **1942**, *13*, 524.
[24] Y. H. Lee, G. T. Tao, *Adv. Biochem. Eng.* **1979**, *13*, 36.
[25] H. Baumgärtl, D. W. Lübbers in *Polarographic Oxygen Sensors* (Eds.: E. Gnaiger, H. Forstner), Springer, Berlin, **1983**, p. 37.
[26] A. M. Bond, T. F. Man, *Electrochim. Acta.* **1987**, *32*, 863.
[27] A. M. Bond, M. Fleischmann, J. Robinson, *J. Electroanal. Chem.* **1984**, *180*, 257.
[28] J. Ghorogchian, F. Sarfarazi, T. Dibble, J. Cassidy, J.-J. Smith, A. Russell, G. Dunmore, M. Fleischmann, S. Pons, *Anal. Chem.* **1986**, *58*, 2278.
[29] A. J. Bard, F.-R. F. Fan, J. Kwak, O. Lev, *Anal. Chem.* **1989**, *61*, 132.
[30] a) R. M. Wightman, D. O. Wipf in *Electroanalytical Chemistry, Vol. 15* (Ed.: A. J. Bard), Marcel Dekker, New York, **1989**, p. 267; b) A. M. Bond, K. B. Oldham, C. G. Zoski, *Anal. Chim. Acta.* **1989**, *216*, 177; c) J. Robinson in *Comprehensive Kinetics, Vol. 29* (Ed.: C. H. Bamford, R. G. Compton), Elsevier, Amsterdam, **1989**, p. 149; d) J. Heinze, *Angew. Chem.* **1991**, *103*, 175; *Angew. Chem. Int. Ed. Engl.* **1991**, *30*, 170; e) R. M. Penner, N. S. Lewis, *Chem. Ind.* **1991**, 788; f) B. R. Scharifker in *Microelectrode Techniques in Electrochemistry Mod. Aspects of Electrochem.)* **1992**, *22*.
[31] a) M. Fleischmann, S. Pons, D. R. Rolison in *Ultramicroelectrodes* (Ed.: P. P. Schmidt), Datatech Systems. Inc. Morganton, **1987**; b) *Microelectrodes: Theory and Application* (Ed.: M. I. Montenegro, M. A. Queiros, J. L. Daschbach) (*NATO ASI Ser. Ser. E* **1991**, *197*).
[32] A. J. Bard, L. R. Faulkner, *Electrochemical Methods, Fundamentals and Applications*, Wiley, New York, **1980**.
[33] A. T. Hubbard, F. C. Anson, *Electroanal. Chem.* **1970**, *4*, 129.
[34] J. Heinze, *Angew. Chem.* **1984**, *96*, 823; *Angew. Chem. Int. Ed. Engl.* **1984**, *23*, 831.
[35] J. Crank, *The Mathematics of Diffusion*, Clarendon, Oxford, **1976**.
[36] A. M. Bond, M. Fleischmann, J. Robinson, *J. Electroanal. Chem.* **1984**, *168*, 299.
[37] M. A. Dayton, J. C. Brown, K. J. Stutts, R. M. Wightman, *Anal. Chem.* **1980**, *52*, 946.
[38] J. O. Howell, R. M. Wightman, *Anal. Chem.* **1984**, *56*, 524.
[39] K. R. Wehmeyer, M. R. Deakin, R. M. Wightman, *Anal. Chem.* **1985**, *57*, 1913.
[40] T. V. Shea, A. J. Bard, *Anal. Chem.* **1987**, *59*, 2101.
[41] P. M. Kovach, W. L. Caudill, D. G. Peters, R. M. Wightman, *J. Electroanal. Chem.* **1985**, *185*, 285.
[42] J. S. Symanski, S. Bruckenstein, *J. Electrochem. Soc.* **1984**, *131*, 110C.
[43] D. R. MacFarlane, D. K. Y. Wong, *J. Electroanal. Chem.* **1985**, *185*, 197.
[44] M. Fleischmann, S. Bandyopadhyay, S. Pons, *J. Phys. Chem.* **1985**, *89*, 5537.
[45] T. Gueshi, K. Tokuda, H. Matsuda, *J. Electroanal. Chem.* **1978**, *89*, 247; *ibid.* **1979**, *101*, 29; *ibid.* **1979**, *102*, 41.
[46] F. Belal, J. L. Anderson, *Analyst* **1985**, *110*, 1493.
[47] M. Ciszkowska, Z. Stojek, *J. Electroanal. Chem.* **1985**, *191*, 101.
[48] H. Reller, E. Kirowa-Eisner, E. Gileadi, *J. Electroanal. Chem.* **1982**, *138*, 65; *ibid.* **1984**, *161*, 247.
[49] D. Shoup, A. Szabo, *J. Electroanal. Chem.* **1984**, *160*, 19.
[50] K. R. Wehmeyer, R. M. Wightman, *Anal. Chem.* **1985**, *57*, 1989.
[51] P. M. Kovach, M. R. Deakin, R. M. Wightman, *J. Phys. Chem.* **1986**, *90*, 4612.
[52] J. Heinze, *J. Electroanal. Chem.* **1981**, *124*, 73.
[53] a) K. Aoki, J. Osteryoung, *J. Electroanal. Chem.* **1981**, *122*, 19; b) K. Aoki, J. Osteryoung, *ibid.* **1984**, *160*, 335.
[54] D. Shoup, A. Szabo, *J. Electroanal. Chem.* **1982**, *140*, 237.
[55] K. B. Oldham, *J. Electroanal. Chem.* **1981**, *122*, 1.
[56] K. B. Oldham, C. G. Zoski, *J. Electroanal. Chem.* **1988**, *256*, 11.
[57] C. G. Zoski, A. M. Bond, E. T. Allinson, K. B. Oldham, *Anal. Chem.* **1990**, *62*, 37.
[58] a) M. Fleischmann, S. Pons, *J. Electroanal. Chem.* **1987**, *222*, 107; b) A. Szabo, *J. Phys. Chem.* **1987**, *91*, 3108.
[59] a) S. Coen, D. K. Cope, D. E. Tallman, *J. Electroanal. Chem.* **1986**, *215*, 29; b) K. Aoki, K. Tokuda, H. Matsuda, *ibid.* **1987**, *225*, 19.
[60] a) J. Heinze, M. Störzbach, *Ber. Bunsenges. Phys. Chem.* **1986**, *90*, 1043; b) M. Störzbach, J. Heinze, *J. Electroanal. Chem.* **1993**, *346*, 1.
[61] a) C. A. Amatore, M. R. Deakin, R. M. Wightman, *J. Electroanal. Chem.* **1986**, *206*, 23; b) M. R. Deakin, R. M. Wightman, C. A. Amatore, *ibid.* **1986**, *215*, 49; c) C. A. Amatore, B. Fosset, M. R. Deakin, R. M. Wightman, *ibid.* **1987**, *225*, 33; d) C. Michael, R. M. Wightman, C. A. Amatore, *ibid.* **1989**, *267*, 33.
[62] W. H. Reinmuth, *J. Am. Chem. Soc.* **1957**, *79*, 6358.
[63] a) K. B. Oldham, C. G. Zoski, A. M. Bond, D. Sweigart, *J. Electroanal. Chem.* **1988**, *248*, 467; b) K. B. Oldham, J. C. Myland, C. G. Zoski, A. M. Bond, *ibid.* **1989**, *270*, 79; c) Z. Galus, J. Golas, J. Osteryoung, *J. Phys. Chem.* **1988**, *92*, 1103.
[64] a) J. Heinze, in [31b], 283); b) M. Störzbach, Disseration, Freiburg, **1991**.
[65] J. C. Imbeaux, J. M. Saveant, *J. Electroanal. Chem.* **1970**, *28*, 325.
[66] J. A. Frauenhofer, C. H. Bank, *Potentostats and its Applications*, Butterworth, London, **1972**.
[67] a) D. Britz, *J. Electroanal. Chem.* **1978**, *88*, 309; b) D. Garreau, J.-M. Saveant, *ibid.* **1974**, *50*, 1.
[68] a) K. B. Oldham, *J. Electroanal. Chem.* **1987**, *237*, 303; b) S. Bruckenstein, *Anal. Chem.* **1987**, *59*, 2098.
[69] A. M. Bond, D. Luscombe, K. B. Oldham, C. G. Zoski, *J. Electroanal. Chem.* **1988**, *249*, 1.
[70] a) K. B. Oldham, C. G. Zoski in *Comprehensive Kinetics, Vol. 26* (Eds.: G. H. Bamford, R. G. Compton), Elsevier, Amsterdam, **1986**, p. 79; b) C. A. Amatore, M. R. Deakin, R. M. Wightman, *J. Electroanal. Chem.* **1987**, *220*, 49.
[71] a) K. B. Oldham in ref. [30b], p. 83; b) K. B. Oldham, *J. Electroanal. Chem.* **1988**, *250*, 1.
[72] M. Fleischmann, F. Lasserre, J. Robinson, *J. Electroanal. Chem.* **1984**, *177*, *115*.
[73] K. B. Oldham, *J. Electroanal. Chem.* **1991**, *313*, 3.
[74] M. Fleischmann, F. Lasserre, J. Robinson, D. Swan, *J. Electroanal. Chem.* **1984**, *177*, 97.
[75] a) A. Denault, M. Fleischmann, D. Pletcher, O. R. Tutty, *J. Electroanal. Chem.* **1990**, *280*, 243; b) A. Denault, M. Fleischmann, D. Pletcher, *J. Electroanal. Chem.* **1990**, *280*, 255; c) A. Denault, D. Pletcher, *ibid.* **1991**, *305*, 131; C. G. Philips, *ibid.* **1990**, *296*, 255.
[76] M. A. Dayton, A. S. Ewing, R. M. Wightman, *Anal. Chem.* **1980**, *52*, 2392.

[77] a) M. Dong, G. Che, *J. Electroanal. Chem.* **1991**, *309*, 103; b) C. L. Miaw, J. F. Rusling, A. Owlia, *Anal. Chem.* **1990**, *62*, 268.
[78] C. G. Zoski, D. A. Sweigart, N. J. Stone, P. H. Reiger, E. Mocellin, T. F. Mann, D. R. Mann, D. K. Gosser, M. M. Doeff, A. M. Bond, *J. Am. Chem. Soc.* **1988**, *110*, 2109.
[79] A. M. Bond, G. Jaouen, T. F. Mann, E. Mocellin, S. Top, *Organometallics* **1989**, *8*, 2382.
[80] a) J. Heinze, M. Störzbach in ref. [31 b], p. 99; b) M. Störzbach, Dissertation, Freiburg, **1991**.
[81] a) L. S. Marcoux, R. N. Adams, S. W. Feldberg, *J. Phys. Chem.* **1969**, *73*, 2611; b) K. Debrodt, K. Heussler, *Z. Phys. Chem. (Munich)* **1981**, *125*, 35.
[82] M. I. Montenegro in ref. [31 b], p. 429.
[83] M. I. Montenegro, D. Pletcher, *J. Electroanal. Chem.* **1988**, *248*, 229.
[84] M. J. Medeiros, M. I. Montenegro, D. Pletcher, *J. Electroanal. Chem.* **1990**, *290*, 155.
[85] M. I. Montenegro, D. Pletcher, E. A. Liolios, D. J. Mazur, C. Zawodzinski, *J. Appl. Electrochem.* **1990**, *20*, 54.
[86] a) S. Dong, G. Che, *J. Electroanal. Chem.* **1991**, *315*, 191; b) G. Che, S. Dong, *Electrochim. Acta* **1992**, *37*, 2695, 2701.
[87] M. Kalaji, L. Nyholm, L. M. Peter, *J. Electroanal. Chem.* **1992**, *325*, 269.
[88] R. John, G. G. Wallace, *J. Electroanal. Chem.* **1991**, *306*, 157.
[89] a) S. U. Pedersen, K. Daasbjerg, *Acta Chem. Scand.* **1989**, *43*, 301; b) K. Daasbjerg, S. U. Pedersen, H. Lund, *ibid.* **1989**, *43*, 875.
[90] C. D. Baer, N. J. Stome, D. A. Sweigart, *Anal. Chem.* **1988**, *60*, 188.
[91] J. D. Norton, H. S. White, S. W. Feldberg, *J. Phys. Chem.* **1990**, *94*, 6772.
[92] K. Itaya, T. Abe, I. Uchida, *J. Electrochem. Soc.* **1987**, *134*, 1191.
[93] B. D. Pendley, H. D. Abruna, *Anal. Chem.* **1990**, *62*, 782.
[94] a) R. M. Penner, M. J. Herben, N. S. Lewis, *Anal. Chem.* **1989**, *61*, 1630; b) R. M. Penner, M. J. Herben, T. L. Longin, N. S. Lewis, *Science*, **1990**, *250*, 1118.
[95] A. M. Bond, T. I. Henderson, D. R. Mann, T. F. Mann, W. Thormann, C. G. Zoski, *Anal. Chem.* **1988**, *60*, 1678.
[96] R. A. Marcus, *J. Phys. Chem.* **1963**, *67*, 853. Nobel-Vortrag: R. A. Marcus, *Angew. Chem.* **1993**, *105*, 1161; *Angew. Chem. Int. Ed. Engl.* **1993**, *32*, 1111.
[97] A. S. Baranski, *J. Electroanal. Chem.* **1991**, *307*, 287.
[98] J. C. Myland, K. B. Oldham, *J. Electroanal. Chem.* **1983**, *147*, 295.
[99] B. Speiser, S. Pons, *Can. J. Chem.* **1982**, *60*, 1352.
[100] I. Lavagnini, P. Pastore, F. Magno, *Can. J. Chem.* **1992**, *333*, 1.
[101] A. Neudeck, J. Dittrich, *J. Electroanal. Chem.* **1991**, *313*, 37.
[102] L. K. Safford, M. J. Weaver, *J. Electroanal. Chem.* **1991**, *312*, 69.
[103] R. S. Nicholson, *Anal. Chem.* **1965**, *37*, 1351.
[104] C. A. Amatore, C. Lefrou, *J. Electroanal. Chem.* **1990**, *296*, 335.
[105] R. M. Wightman, D. O. Wipf, *Acc. Chem. Res.* **1990**, *23*, 64.
[106] J. W. Howell, R. M. Wightman, *J. Phys. Chem.* **1984**, *88*, 3915.
[107] J. O. Howell, J. Goncalves, C. Amatore, L. Klasinc, J. Kochi, R. M. Wightman, *J. Am. Chem. Soc.* **1984**, *106*, 3968.
[108] P. Hapiot, J. Pinson, C. Francesch, F. Mhamdi, C. Rolando, S. Schneider, *J. Electroanal. Chem.* **1992**, *328*, 327.
[109] M. I. Montenegro, D. Pletcher, *J. Electroanal. Chem.* **1986**, *200*, 371.
[110] C. P. Andrieux, P. Hapiot, J.-M. Saveant, *Chem. Rev.* **1990**, *90*, 723.
[111] W. J. Bowyer, D. H. Evans, *J. Org. Chem.* **1988**, *53*, 5234.
[112] a) D. O. Wipf, R. M. Wightman, *Anal. Chem.* **1988**, *60*, 2460; b) D. O. Wipf, R. M. Wightman, *J. Phys. Chem.* **1989**, *93*, 4286.
[113] a) R. S. Robinson, R. L. McCreery, *Anal. Chem.* **1981**, *53*, 997; b) R. S. Robinson, C. W. McCurdy, R. L. McCreery, *ibid.* **1982**, *54*, 2356; c) R. S. Robinson, R. L. McCreery, *J. Electroanal. Chem.* **1985**, *182*, 61.
[114] K. Meerholz, P. Tschuncky, J. Heinze, *J. Electroanal. Chem.* **1993**, *347*, 425.
[115] a) A. Fitch, D. H. Evans, *J. Electroanal. Chem.* **1986**, *202*, 83; b) W.-J. Boyer, D. H. Evans, *ibid.* **1988**, *240*, 227.
[116] a) D. Larumbe, I. Gallando, C. P. Andrieux, *J. Electroanal. Chem.* **1991**, *304*, 241; b) H. Yang, D. O. Wipf, A. J. Bard, *ibid.* **1992**, *331*, 913; c) C. A. Amatore, A. Jutan, F. Pflüger, *ibid.* **1987**, *218*, 361.
[117] C. P. Andrieux, P. Hapiot, J.-M. Saveant, *J. Phys. Chem.* **1988**, *92*, 5987; *ibid.* **1988**, *92*, 5992.
[118] H. Taube, H. Myers, *J. Am. Chem. Soc.* **1954**, *76*, 2103.
[119] C. P. Andrieux, P. Audebert, P. Hapiot, J.-M. Saveant, *J. Am. Chem. Soc.* **1990**, *112*, 2439.
[120] a) P. Tschuncky, J. Heinze, *Synth. Met.* **1993**, *55*, 1603; b) P. Tschuncky, Diplomarbeit, Freiburg, **1991**; P. Tschuncky, J. Heinze, unpublished results.
[121] C. A. Amatore, C. Lefrou, F. Pflüger, *J. Electroanal. Chem.* **1989**, *270*, 43.
[122] a) C. P. Andrieux, D. Garreau, P. Hapiot, J. Pinson, J.-M. Saveant, *J. Electroanal. Chem.* **1988**, *243*, 321; b) C. P. Andrieux, D. Garreau, P. Hapiot, J.-M. Saveant, *ibid.* **1988**, *248*, 447; c) D. Garreau, P. Hapiot, J.-M. Saveant, *ibid.* **1989**, *272*, 1; d) D. Garreau, P. Hapiot, J.-M. Saveant, *ibid.* **1990**, *289*, 73.
[123] G. M. Brisard, M. Manzini, A. Lasia, *J. Electroanal. Chem.* **1992**, *326*, 317.
[124] W. J. Bowyer, E. E. Engelman, D. H. Evans, *J. Electroanal. Chem.* **1989**, *262*, 67.
[125] D. W. Wipf, E. W. Kristensen, M. R. Deakin, R. M. Wightman, *Anal. Chem.* **1988**, *60*, 306.
[126] L. K. Safford, M. J. Weaver, *J. Electroanal. Chem.* **1992**, *331*, 857.
[127] N. Oyama, S. Kikuyama, T. Tatsuma, *J. Electroanal. Chem.* **1993**, *344*, 367.
[128] A. S. Baranski, K. Winkler, W. R. Fawcett, *J. Electroanal. Chem.* **1991**, *313*, 367.
[129] D. O. Wipf, A. C. Michael, R. M. Wightman, *J. Electroanal. Chem.* **1989**, *269*, 15.
[130] a) K. Nuzaki, M. Oyama, H. Hatano, S. Okazaki, *J. Electroanal. Chem.* **1989**, *270*, 191; b) S. Nomura, K. Nozaki, S. Okazaki, *Anal. Chem.* **1991**, *63*, 2665.
[131] C. A. Amatore, C. Lefrou, *J. Electroanal. Chem.* **1992**, *324*, 33.
[132] J. O. Howell, W. G. Kuhr, R. E. Ensman, R. M. Wightman, *J. Electroanal. Chem.* **1986**, *209*, 77.
[133] a) W. Thormann, P. van den Bosch, A. M. Bond, *Anal. Chem.* **1985**, *57*, 2764; b) A. M. Bond, T. L. E. Henderson, W. Thormann, *J. Phys. Chem.* **1986**, *90*, 2911.
[134] A. M. Bond, P. A. Lay, *J. Electroanal. Chem.* **1986**, *199*, 285.
[135] a) J. B. Cooper, A. M. Bond, *J. Electroanal. Chem.* **1991**, *315*, 143; b) J. B. Cooper, A. M. Bond, K. B. Oldham, *ibid.* **1992**, *331*, 877.
[136] J. D. Norton, H. S. White, *J. Electroanal. Chem.* **1992**, *325*, 341.
[137] a) C. A. Amatore, B. Fosset, J. Bartelt, M. R. Deakin, R. M. Wightman, *J. Electroanal. Chem.* **1988**, *256*, 255; b) S. M. Drew, R. M. Wightman, C. A. Amatore, *ibid.* **1991**, *317*, 117.
[138] a) M. Ciszkowska, Z. Stojek, *J. Electroanal. Chem.* **1986**, *213*, 189; b) Z. Stojek, J. Osteryoung, *Anal. Chem.* **1988**, *60*, 131; c) M. Ciszkowska, Z. Stojek, J. Osteryoung, *ibid.* **1990**, *62*, 349.
[139] C. Lea, F. C. Anson, *J. Electroanal. Chem.* **1992**, *323*, 381.
[140] A. M. Bond, M. Fleischmann, J. Robinson, *J. Electroanal. Chem.* **1984**, *172*, 11.
[141] a) J. D. Norton, W. E. Benson, H. S. White, B. D. Pendley, H. D. Abruna, *Anal. Chem.* **1991**, *63*, 1909; b) B. D. Pendley, H. D. Abruna, J. D. Norton, W. E. Benson, H. S. White, *ibid.* **1991**, *63*, 2766.
[142] J. Cassidy, S. B. Khoo, S. Pons, M. Fleischmann, *J. Phys. Chem.* **1985**, *89*, 3933.
[143] C. Jehoulet, A. J. Bard, *Angew. Chem.* **1991**, *103*, 882; *Angew. Chem. Int. Ed. Engl.* **1991**, *30*, 836.
[144] a) L. Geng, A. G. Ewing, J. C. Jernigan, R. W. Murray, *Anal. Chem.* **1986**, *58*, 85; b) L. Geng, R. W. Murray, *Inorg. Chem.* **1986**, *25*, 311.
[145] S. Nakabayashi, A. Fujishima, K. Honda, *J. Electroanal. Chem.* **1980**, *111*, 391; *ibid.* **1983**, *149*, 149.
[146] M. V. Novotny, S. R. Springston, P. A. Peaden, J. C. Fjeldsted, M. L. Lee, *Anal. Chem.* **1981**, *53*, 407A.
[147] a) M. E. Philips, M. R. Deakin, M. V. Novotny, R. M. Wightman, *J. Phys. Chem.* **1987**, *91*, 3934; b) D. Niehaus, M. Philips, A. Michael, R. M. Wightman, *ibid.* **1989**, *93*, 6232; c) A. C. Michael, R. M. Wightman, *Anal. Chem.* **1989**, *61*, 2193; *ibid.* **1989**, *61*, 2770.
[148] W. Gorski, J. A. Cox, *J. Electroanal. Chem.* **1992**, *323*, 163.
[149] a) R. A. Reed, L. Geng, R. W. Murray, *J. Electroanal. Chem.* **1986**, *208*, 185; b) L. Geng, R. A. Reed, R. W. Murray, *J. Phys. Chem.* **1987**, *91*, 2914; c) L. Geng, R. A. Reed, M.-H. King, T. T. Wooster, B. N. Oliver, J. Egekeze, R. T. Kennedy, J. W. Jorgenson, J. F. Parcher, R. W. Murray, *J. Am. Chem. Soc.* **1989**, *111*, 1614; d) R. A. Reed, T. T. Wooster, R. W. Murray, D. R. Yaniv, J. S. Tonge, D. F. Shriver, *J. Electrochem. Soc.* **1989**, *136*, 2565; e) H. Nishihara, F. Dalton, W. Murray, *Anal. Chem.* **1991**, *63*, 2955; f) T. T. Wooster, M. L. Longmine, H. Zhang, M. Watanabe, R. W. Murray, *ibid.* **1992**, *64*, 1132.
[150] a) A. M. Bond, M. Svestka, *J. Electroanal. Chem.* **1991**, *301*, 139; b) A. M. Bond, V. B. Pfund, *ibid.* **1992**, *325*, 281.
[151] D. K. Gosser, Q. Huang, *J. Electroanal. Chem.* **1989**, *267*, 333.
[152] a) R. Brina, S. Pons, M. Fleischmann, *J. Electroanal. Chem.* **1988**, *244*, 81; b) R. Brina, S. Pons, *ibid.* **1989**, *264*, 121.
[153] J. Ghoroghchian, S. Pons, M. Fleischmann, *J. Electroanal. Chem.* **1991**, *317*, 101.
[154] a) H. Baumgärtl, D. W. Lübbers in *Oxygen Supply* (Eds.: M. Kessler, D. F. Bruley, L. C. Clark, D. W. Lübbers, I. A. Silver, J. Strauss), Urban und Schwarzenberg, München, **1973**, p. 130–136; b) H. Baumgärtl in *Clinical Oxygen Measurement* (Eds.: A. M. Ehrly, J. Hauss, R. Huch), Springer, Heidelberg, **1987**, p. 17–42; c) H. Baumgärtl, U. Heinrich, D. W. Lübbers, *Pfluegers Arch.* **1989**, *414*, 228; d) J. Beunink, H. Baumgärtl, W. Zimelka, H.-J. Rehm, *Experientia* **1989**, *45*, 1041.
[155] a) R. N. Adams, *Anal. Chem.* **1976**, *48*, 1126A; b) R. M. Wightman, E. Strope, P. M. Plotsky, R. N. Adams, *Nature* **1976**, *262*, 145.
[156] a) R. Kelly, R. M. Wightman, *Anal. Chim. Acta* **1986**, *187*, 79; E. W. Kristensen, W. G. Kuhr, R. M. Wightman, *Anal. Chem.* **1987**, *59*, 1751; J. E. Baur, E. W. Kristensen, L. J. May, D. J. Wiedemann, R. M. Wightman, *ibid.* **1988**, *60*, 1268.
[157] B. Poulain, G. Baux, L. Tauc, D. Henzel, *Anal. Chem.* **1986**, *58*, 2091.
[158] P. A. Broderick, *Electroanalysis* **1990**, *2*, 241.
[159] a) M. Armstrong-James, K. Fox, Z. I. Kruk, J. Millar, *J. Neurosci. Methods* **1981**, *4*, 385; b) W. G. Kuhr, R. M. Wightman, *Brain Res.* **1986**, *381*, 168; c) D. J. Wiedemann, K. T. Kawagoe, R. T. Kennedy, E. Ciolkowski, R. M. Wightman, *Anal. Chem.* **1991**, *63*, 2965.

[160] a) T. K. Chen, Y. Y. Lau, D. K. Y. Wong, A. G. Ewing, *Anal. Chem.* **1992**, *64*, 1264; b) F. Bailey, T. Malinski, F. Kiechle, *ibid.* **1991**, *63*, 395.
[161] a) R. M. Wightman, L. J. May, A. C. Michael, *Anal. Chem.* **1988**, *60*, 769A; b) R. M. Wightman, R. T. Kennedy, D. J. Wiedemann, K. T. Kawagoe, J. B. Zimmerman, D. J. Leszczyszyn in ref. [30b], p. 453M; c) K. T. Kawagoe, J. A. Jankowski, R. M. Wightman, *Anal. Chem.* **1991**, *63*, 1589.
[162] W. P. Hamil, A. Marty, E. Neher, B. Sakmann, F. J. Sigworth, *Pfluegers Arch.* **1981**, *391*, 85.
[163] a) E. Neher, *Angew. Chem.* **1992**, *104*, 837; *Angew. Chem. Int. Ed. Engl.* **1992**, *31*, 824; b) B. Sakmann, *ibid.* **1992**, *104*, 844 or **1992**, *31*, 830.
[164] L. von Rüden, H. Chow, E. Neher, *Tagungsband DECHEMA* Symp. Mikroelektrochemie, Friedrichroda, **1992**.
[165] a) K. Bade, V. Tsakova, J. W. Schulze, *Electrochim. Acta* **1992**, *37*, 2255; b) M. Fleischmann, S. Pons, J. Daschbach in ref. [31b], p. 393.
[166] a) R. L. Deutscher, S. Fletcher, *J. Electroanal. Chem.* **1988**, *239*, 17; *ibid.* **1990**, *270*, 1; b) S. Fletcher in ref. [31b], p. 341.
[167] a) C. L. Colyer, D. Luscombe, K. B. Oldham, *J. Electroanal. Chem.* **1990**, *283*, 379; b) C. L. Colyer, K. B. Oldham, S. Fletcher, *ibid.* **1990**, *290*, 33.
[168] H. S. Isaacs, *J. Electrochem. Soc.* **1988**, *135*, 2180.
[169] a) R. C. Newman, *Corros. Sci.* **1985**, *25*, 341; b) R. T. Atanasoski, H. S. White, W. H. Smyrl, *J. Electrochem. Soc.* **1986**, *133*, 2435; K. Wikiel, J. Osteryoung, *ibid.* **1988**, *135*, 1915.
[170] a) D. E. Williams, C. Westcott, M. Fleischmann, *J. Electroanal. Chem.* **1985**, *132*, 1796; *ibid.* **1985**, *132*, 1804; b) D. E. Williams, in ref. [31b], p. 445.
[171] a) G. Binning, H. Rohrer, *Angew. Chem.* **1987**, *99*, 622; *Angew. Chem. Int. Ed. Engl.* **1987**, *26*, 606; b) J. Frommer, *ibid.* **1992**, *104*, 1325 or **1992**, *32*, 1298.
[172] a) A. J. Bard, F.-R. R. Fan, J. Kwak, O. Lev, *Anal. Chem.* **1989**, *61*, 132; b) A. J. Bard, G. Denuault, C. Lee, D. Mandler, D. O. Wipf, *Acc. Chem. Res.* **1990**, *23*, 357; c) A. J. Bard, F.-R. F. Fan, D. T. Pierce, P. R. Unwin, D. O. Wipf, F. Zhou, *Science* **1991**, *254*, 68.
[173] J. Kwak, A. J. Bard, *Anal. Chem.* **1989**, *61*, 1221.
[174] a) J. Kwak, A. J. Bard, *Anal. Chem.* **1989**, *61*, 1794; b) C. Lee, C. J. Miller, A. J. Bard, *ibid.* **1991**, *63*, 78.
[175] C. Lee, A. J. Bard, *Anal. Chem.* **1990**, *62*, 1906.
[176] J. Kwak, C. Lee, A. J. Bard, *J. Electrochem. Soc.* **1990**, *137*, 1481.
[177] C. Lee, J. Kwak, A. J. Bard, *Proc. Natl. Acad. Sci. USA* **1990**, *87*, 1740.
[178] D. O. Wipf, A. J. Bard, *J. Electrochem. Soc.* **1991**, *138*, 469.
[179] R. C. Engstrom, B. Small, L. Kattan, *Anal. Chem.* **1992**, *64*, 241.
[180] J. Wang, L.-H. Wu, R. Li, *J. Electroanal. Chem.* **1989**, *272*, 285.
[181] a) R. C. Engstrom, M. Weber, D. J. Wunder, R. Burgess, S. Winquist, *Anal. Chem.* **1986**, *58*, 844; b) R. C. Engstrom, T. Meaney, R. Tople, R. M. Wightman, *ibid.* **1987**, *59*, 2005; R. C. Engstrom, R. M. Wightman, E. W. Kristensen, *ibid.* **1988**, *60*, 652.
[182] W. J. Albery, M. L. Hitchman, *Ring-Disc-Electrodes*, Clarendon, Oxford, **1971**.
[183] C. Lee, J. Kwak, F. C. Anson, *Anal. Chem.* **1991**, *63*, 1501.
[184] a) D. H. Craston, C. W. Lin, A. J. Bard, *J. Electrochem. Soc.* **1988**, *135*, 785; b) O. E. Hüsser, D. H. Craston, A. J. Bard, *J. Vac. Sci. Technol. B* **1988**, *6*, 1873; c) O. E. Hüsser, D. H. Craston, A. J. Bard, *J. Electrochem. Soc.* **1989**, *136*, 3222; d) T.-M. Wuu, F.-R. F. Fan, A. J. Bard, *ibid.* **1989**, *136*, 885.
[185] a) D. Mandler, A. J. Bard, *J. Electrochem. Soc.* **1989**, *136*, 3143; b) *ibid.* **1990**, *137*, 1079; c) *ibid.* **1990**, *137*, 2468.
[186] a) C. Lee, D. O. Wipf, A. J. Bard, K. Bartels, A. C. Bovik, *J. Electrochem. Soc.* **1991**, *63*, 2442; b) D. O. Wipf, A. J. Bard, *ibid.* **1992**, *64*, 1362.
[187] A. J. Bard, J. A. Crayston, G. P. Kittlesen, T. V. Shea, M. S. Wrighton, *Anal. Chem.* **1986**, *58*, 231.
[188] C. E. Chidsey, B. J. Feldman, C. Lundgren, R. W. Murray, *Anal. Chem.* **1986**, *58*, 601.
[189] a) J. E. Bartelt, M. R. Deakin, C. Amatore, R. M. Wightman, *Anal. Chem.* **1988**, *60*, 2167; b) B. Fosset, C. Amatore, J. Bartelt, R. M. Wightman, *ibid.* **1991**, *63*, 1403.
[190] O. Niwa, M. Morita, H. Tabei, *Anal. Chem.* **1990**, *62*, 447.
[191] W. F. Berry, S. G. Weber, *J. Electroanal. Chem.* **1986**, *208*, 77.
[192] D. J. Wiedemann, K. T. Kawagoe, R. T. Kennedy, E. L. Ciolkowski, R. M. Wightman, *Anal. Chem.* **1991**, *63*, 2965.
[193] a) D. P. Whelan, J. J. O'Dea, J. Osteryoung, *J. Electroanal. Chem.* **1986**, *202*, 23; b) J. J. O'Dea, M. Wojciechowski, J. Osteryoung, *Anal. Chem.* **1985**, *57*, 954; c) K. Aoki, K. Tokuda, H. Matsuda, J. Osteryoung, *J. Electroanal. Chem.* **1986**, *207*, 25; d) L. Sinru, J. Osteryoung, J. J. O'Dea, R. Osteryoung, *Anal. Chem.* **1988**, *60*, 1135; e) M. J. Nuwer, J. Osteryoung, *ibid.* **1989**, *61*, 1954; f) C. Wechter, J. Osteryoung, *ibid.* **1989**, *61*, 2092; g) J. Osteryoung, M. M. Murphy, in ref. [30b], p. 123; h) J. Osteryoung in ref. [31b], p. 139.
[194] A. G. Ewing, M. A. Dayton, R. M. Wightman, *Anal. Chem.* **1981**, *53*, 1842.
[195] a) F. G. Gonon, C. M. Fombarlet, M. J. Buda, J. F. Pujol, *Anal. Chem.* **1981**, *53*, 1386; b) F. G. Gonon, F. Navarre, M. J. Buda, *ibid.* **1984**, *56*, 573.
[196] a) S. A. Schuette, R. L. McCreery, *J. Electroanal. Chem.* **1985**, *191*, 329; b) S. A. Schuette, R. L. McCreery, *Anal. Chem.* **1986**, *58*, 1778.
[197] a) A. S. Baranski, H. Quon, *Anal. Chem.* **1986**, *58*, 407; b) A. S. Baranski, *ibid.* **1987**, *59*, 662.
[198] C. Wechter, J. Osteryoung, *Anal. Chem.* **1989**, *61*, 2092.
[199] J. F. Coetzee, M. J. Ecoff, *Anal. Chem.* **1991**, *63*, 957.
[200] a) D. C. Johnson, S. G. Weber, A. M. Bond, R. M. Wightman, R. E. Shoup, I. S. Krull, *Anal. Chim. Acta* **1986**, *180*, 187; J. W. Bixler, A. M. Bond, *Anal. Chem.* **1986**, *58*, 2859; c) L. A. Knecht, E. J. Guthrie, J. W. Jorgenson, *ibid.* **1984**, *56*, 479; d) J. W. Bixler, M. Fifield, J. C. Poler, A. M. Bond, W. Thormann, *Electroanalysis* **1989**, *1*, 23; e) J. L. Anderson, K. K. Whiten, J. D. Brewster, T. Y. Ou, W. K. Nonidez, *Anal. Chem.* **1985**, *57*, 1366; f) M. Takahashi, M. Morita, O. Niwa, H. Tabei, *J. Electroanal. Chem.* **1992**, *335*, 253.
[201] J. M. Zadeii, R. Mitchell, T. Kuwana, *Electroanalysis* **1990**, *2*, 209.
[202] A. Aoki, T. Matsue, I. Uchida, *Anal. Chem.* **1992**, *64*, 44.
[203] D. H. Craston, C. P. Jones, D. E. Williams, *Talanta* **1991**, *38*, 17.
[204] a) S. T. Singleton, J. O'Dea, J. Osteryoung, *Anal. Chem.* **1989**, *61*, 1211; b) M. M. Murphy, J. O'Dea, J. Osteryoung, *ibid.* **1991**, *63*, 2743.
[205] N. Sleszynski, J. Osteryoung, M. Carter, *Anal. Chem.* **1984**, *56*, 130.
[206] D. E. Williams, in ref. [31b], p. 415.
[207] K. Camman, U. Lemke, A. Rohen, J. Sander, H. Wilken, B. Winter, *Angew. Chem.* **1991**, *103*, 519; *Angew. Chem. Int. Ed. Engl.* **1991**, *30*, 516.
[208] T. Zeuthen, *Med. Biol. Eng.* **1978**, *16*, 489.
[209] S. Fletcher in ref. [31b], p. 243.
[210] P. Tschuncky, J. Heinze, *Anal. Chem.*, submitted.
[211] A. Meulemans, B. Poulain, G. Baux, L. Tauc, D. Hanzel, *Anal. Chem.* **1986**, *58*, 2088.
[212] a) K. Potje-Kamloth, J. Janata, M. Josowicz, *Ber. Bunsenges. Phys. Chem.* **1989**, *93*, 1480; b) K. Potje-Kamloth, J. Janata, M. Josowicz, *Sens. Actuators* **1989**, *18*, 415; c) K. T. Kawagoe, J. A. Jankowski, R. M. Wightman, *Anal. Chem.* **1991**, *63*, 1589.
[213] F. Bailey, T. Malinski, F. Kiechle, *Anal. Chem.* **1991**, *63*, 395.
[214] a) T. G. Strein, A. G. Ewing, *Anal. Chem.* **1991**, *63*, 194; b) T. G. Strein, A. G. Ewing, *ibid.* **1992**, *64*, 1368; c) Y. Y. Lau, T. Abe, A. G. Ewing, *ibid.* **1992**, *64*, 1702.
[215] a) J. O. Besenhard, A. Schulte, K. Schur, P. D. Jannakoudakis, in ref. [30b], p. 189; b) A. Schulte, J. Besenhard, P. D. Jannakoudakis, J. Heinze, P. Tschuncky, *Tagungsband DECHEMA* Symp. *Mikroelektrochemie*, Friedrichroda, **1992**.
[216] G. Mengoli, P. Bianco, S. Dalio, M. T. Munari, *J. Electrochem. Soc.* **1981**, *128*, 2276.
[217] R. L. McCarley, M. G. Sullivan, S. Ching, Y. Zhang, R. W. Murray, in ref. [30b], p. 205.
[218] A. M. Bond, T. L. E. Henderson, W. Thormann, *J. Phys. Chem.* **1986**, *90*, 2911.
[219] a) R. S. Morris, D. J. Franmta, H. S. White, *J. Phys. Chem.* **1987**, *91*, 3559; b) J. B. Seibold, E. R. Scott, H. S. White, *J. Electroanal. Chem.* **1989**, *264*, 281.
[220] K. Aoki, K. R. Tokuda, *J. Electrochem. Chem.* **1987**, *237*, 163.
[221] L. F. Thompson, C. G. Wilson, *Introduction to Microlithography* (Ed.: M. J. Bowden), American Chemical Society, Washington, D.C., **1983**.
[222] a) G. P. Kittlesen, H. S. White, M. S. Wrighton, *J. Am. Chem. Soc.* **1984**, *106*, 7289; b) G. P. Kittlesen, H. S. White, M. S. Wrighton, *ibid.* **1985**, *107*, 7373; c) E. W. Paul, A. J. Ricco, M. S. Wrighton, *J. Phys. Chem.* **1985**, *89*, 1441; d) E. T. Turner Jones, O. M. Chyan, M. S. Wrighton, *J. Am. Chem. Soc.* **1987**, *109*, 5526.
[223] M. Samuelsson, M. Armgarth, C. Nylander, *Anal. Chem.* **1991**, *63*, 931.
[224] J. W. Schultze, *Nachr. Chem. Tech. Lab.* **1993**, *42*, 205.
[225] a) J. W. Schultze, J. Thietke, *Electrochim. Acta* **1989**, *34*, 1769; b) J. W. Schultze, K. Bade, O. Kartens, A. Michaelis, *Ber. Bunsenges. Phys. Chem.* **1991**, *95*, 1350.